JCI insight

Human *C. difficile* toxin-specific memory B cell repertoires encode poorly-neutralizing antibodies

Hemangi B. Shah, … , Jimmy D. Ballard, Mark L. Lang

JCI Insight. 2020. https://doi.org/10.1172/jci.insight.138137.

Research In-Press Preview Immunology Infectious disease

Graphical abstract

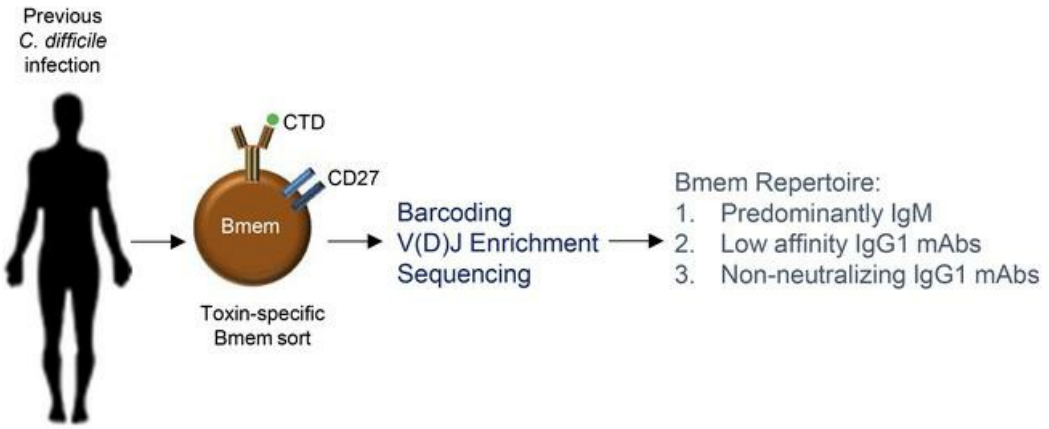

Human *C. difficile* toxin-specific memory B cell repertoires encode poorly-neutralizing antibodies

Hemangi B. Shah[1], Kenneth Smith[2], Edgar J. Scott, II[1^], Jason Larabee[1], Judith A. James[2,3], Jimmy D. Ballard[1] and Mark L. Lang[1]

1. Department of Microbiology and Immunology, University of Oklahoma Health Sciences Center, Oklahoma City, OK, USA.
2. Arthritis and Clinical Immunology, Oklahoma Medical Research Foundation, Oklahoma City, OK, USA.
3. Departments of Medicine and Pathology, University of Oklahoma Health Sciences Center, Oklahoma City, OK, USA.

^Edgar J. Scott, II current affiliation: United States Air Force, 3001 Staff Drive, Tinker Air Force Base, Oklahoma City, OK 73145

Key words: *C. difficile*, memory B cells, antibody repertoire, single-cell sequencing

Corresponding author:
Mark L. Lang, PhD
University Of Oklahoma Health Sciences Center
940 Stanton L. Young Blvd
Oklahoma City, OK 73104 USA
Tel: 405-271-2193
Mark-Lang@ouhsc.edu

Conflict of Interest Statement

The authors have declared that no conflict of interest exists.

ABSTRACT

Clostridioides difficile is a leading cause of nosocomial infection responsible for significant morbidity and mortality with limited options for therapy. Secreted *C. difficile* toxin B (TcdB) is a major contributor to disease pathology and select TcdB-specific Abs may protect against disease recurrence. However, the high frequency of recurrence suggests that the memory B cell response, essential for new Ab production following *C. difficile* re-exposure, is insufficient. We therefore isolated TcdB-specific memory B cells from individuals with a history of *C. difficile* infection and performed single-cell deep sequencing of their Ab genes. Herein, we report that TcdB-specific memory B cell-encoded antibodies showed somatic hypermutation but displayed limited isotype class switch. Memory B cell-encoded monoclonal antibodies generated from the gene sequences revealed low to moderate affinity for TcdB and a limited ability to neutralize TcdB. These findings indicate that memory B cells are an important factor in *C. difficile* disease recurrence.

INTRODUCTION

C. difficile is responsible for almost half a million infections and 30,000 deaths in the US annually [1] and is a significant global health issue [2-5]. *C. difficile* colonization of the large intestine results in symptoms ranging from diarrhea to life-threatening pseudo-membranous colitis, sepsis and even death [6-11]. The causes of *C. difficile* associated mortality are not entirely clear but case reports suggest systemic sequelae of the disease are contributory [12]. Systemic complications of *C. difficile* reported to date include hepatic abscesses [13], ascites [14], pleural effusion and acute respiratory distress [15, 16], and sepsis and multi-organ failure [10].

The enteric and systemic pathology associated with *C. difficile* infection (CDI) is attributable to secreted toxins known as TcdA and TcdB [17-19]. These toxins enter target cells and glucosylate Rho GTPases to facilitate broad cellular damage [20, 21]. Blood-borne TcdA and TcdB can be detected in some patients and are toxic to target cells *in vitro* [22]. However, TcdA-negative strains can also be highly virulent [19, 23] and although there is one recent report of disease associated with a TcdB-negative strain [24], it is clear that TcdB is a major driver of disease. TcdB has systemic toxicity in several animal species [25-28], supporting the observations of systemic pathology in patients.

There are several distinct ribotypes and strains of pathogenic *C. difficile* that cause disease of varying severity [29]. Infection with a hyper-virulent *C. difficile* strain such as the NAP1/027/BI (ribotype 027) is associated with more severe disease than a historical strain such as VPI-10463 (ribotype 003) [30-32]. Mutation of TcdB is likely to contribute to differences in disease severity. Although NAP1/027/BI toxin B (TcdB2) and VPI-10463 toxin B (TcdB1) share 92% sequence identity and are similarly immunogenic [33], TcdB2 is more cytotoxic than TcdB1 [28].

As many as 30% of individuals with an initial CDI will suffer from disease recurrence [34]. There are several risk factors for recurrence including antibiotic use, advanced age, immune

response, and the *C. difficile* strains to which patients are exposed [35-39]. Recurrent CDI is characterized by re-growth of bacteria that have survived antibiotic therapy or by re-infection with *C. difficile* and each recurrence increases the probability of further episodes [40]. Recurrence is associated with progressively worsening pathology and increasing mortality [41].

C. difficile recurrence indicates that an initial infection failed to adequately immunize the individual and confer protection against subsequent infection. Indeed, patients with higher anti-TcdA and –TcdB serum IgG titers have lower rates of recurrence and TcdB-specific IgG is the best known correlate of protection against *C. difficile* [37, 42-45]. For example, in two independent studies of patients with CDI, recruiting 99 and 61 patients respectively, high serum titers of TcdB-binding and/or -neutralizing IgG were associated with a lower rate of disease recurrence [43, 45]. Bacterial load during infection correlates directly with age and inversely with TcdB-neutralizing IgG titers [46]. There is also indirect evidence for protective humoral immunity. CDI risk is increased in HIV-infected individuals with declining $CD4^+$ T helper cell counts [47], and in immunosuppressed organ transplant recipients [48]. The quality of the IgG response is also important for protection, for example the TcdB-neutralizing FDA-approved IgG mAb bezlotoxumab binds TcdB with high affinity [49]. In a clinical trial, of 200 patients (101 on mAb therapy, 99 on placebo), recurrence was cut by approximately 80% [50]. In two subsequent double-blind phase III trials of 2655 patients recurrence was cut by approximately 60% [51]. The binding affinity of mAbs to TcdB has only been examined in the context of therapeutic mAbs thus far and needs to be evaluated for Abs from past CDI patients.

Despite the clear association between TcdB-neutralizing IgG and disease protection, B cell memory following CDI is not well characterized and its consequences for recurrent infection are poorly defined. Antigen-activated B cells can differentiate into short- or long-lived Ab-secreting plasma cells or into memory B (B_{mem}) cells [reviewed in [52, 53]]. Re-stimulation of B_{mem} cells with booster vaccines or repeat infections can drive their differentiation into new Ab-secreting

plasma cells with the added benefit of speed, increased magnitude, prior isotype switch, and somatic hyper-mutation (SHM) to generate high affinity Ab.

Weak toxin-specific Bmem cell responses in individuals with CDI were demonstrated previously by our lab and others [33, 54]. This warrants a detailed analysis of the Bmem-encoded Ab to identify the underlying defects that may prevent an adequate response. We therefore profiled the TcdB-specific Bmem cell repertoire in individuals who had a prior CDI. These individuals self-reported having been diagnosed with CDI with one requiring hospitalization due to CDI. The carboxy-terminal domain (CTD) of TcdB consists of combined repetitive oligopeptides (CROPs) that are known to contain neutralizing epitopes [55, 56]. Although infection with strain VPI-10463 is unlikely, the antibodies (Abs) to TcdB1 and TcdB2 are highly cross-reactive [57]. We therefore used fluorophore-conjugated CTD (amino acids 1651-2366) of TcdB1 to identify specific Bmem cells in the PBMC of individuals with a history of CDI. Using single-cell barcoding and deep sequencing of bulk sorted CTD-specific Bmem cells, we generated several hundred complete Ab gene sequences for 3 individuals. Analysis of the Ab features revealed a low degree of isotype switch with IgM dominating the repertoires. The IgG-encoding Bmem cells demonstrated a high degree of SHM. The IgM, IgA, and IgG repertoires were also dominated by unique clones, indicating very limited clonal expansion. The IgG1 gene sequences were expressed *in vitro* resulting in production of 49 full length, intact IgG1 monoclonal Abs (mAbs). While 50% of the mAbs showed demonstrable binding to TcdB1 and TcdB2 only one mAb neutralized TcdB2 *in vitro*. These data show that the Bmem cell repertoire following CDI encodes affinity-matured Abs that are likely to provide limited protection against TcdB-driven pathogenesis. These results may contribute to an explanation for recurrent disease following CDI.

RESULTS

Detection of CTD-specific Bmem cells in individuals with a history of *C. difficile* infection and preparation for repertoire analysis

Blood samples were collected from study participants described in **Table S1** before enrichment of total B cells (**Figure 1A**). Flow cytometry was performed to identify singlet $CD3^-$, $CD19^+$, $CD20^+$, $CD27^+$, $CD38^-$, CTD^+ Bmem cells and $CD3^-$, $CD19^+$, $CD20^+$, $CD27^+$, $CD38^-$, CTD^- Bmem cells (**Figure 1B**). CTD-binding Bmem cells were typically undetectable or present at very low frequencies in individuals who had no known history of CDI (**Figure 1C**). Therefore, populations of CTD-specific Bmem cells could readily be detected and distinguished from Bmem cells of other specificities. CTD^+ and CTD^- Bmem cells were then sorted and processed as described in methods to generate a library of barcoded Ig sequences that was in turn curated to analyze the CTD-specific Bmem repertoire as well as the total non-specific (CTD^-) repertoire (**Figure 1D**). The full gating strategy for sorting CTD^+ and CTD^- Bmem cells and the specificity of CTD binding to B cell antigen receptors (BCR) is depicted in **Figures S1 and S2**.

In addition to flow cytometry, we used a second method to detect CTD^+ IgG^+ Bmem cells, following polyclonal stimulation *in vitro*. PBMCs isolated from subjects 1008, 1009, 1013 and three other subjects as well as four healthy controls were cultured with polyclonal stimuli to drive differentiation of Bmem cells into new IgG-secreting plasmablasts which could then be detected by ELISPOT (**Figure S2**). The subjects and controls had a similar frequency of total Bmem cell-derived IgG-secreting cells. None of the controls had CTD-specific IgG-secreting cells. Consistent with previous studies, only one of the four subjects (#1008) showed a clearly positive result, with detectable CTD-specific IgG-secreting cells [33, 54]. This shows that CTD^+ Bmem cells had a poor capacity to differentiate into new plasmablasts following polyclonal stimulation *in vitro*.

Lower frequency of class-switch in CTD$^+$ Bmem cells than in CTD$^-$ Bmem cells

Ig / Ab gene sequences from CTD$^+$ and CTD$^-$ Bmem cells from subjects 1008, 1009 and 1013 were analyzed and the heavy chains were grouped according to Ab class and IgG subclass (**Figure 2**). A lower proportion of the CTD$^+$ Bmem cell-encoded Abs were class-switched (to IgA or IgG) as compared to that observed for the CTD$^-$ Bmem cells. For subjects 1008, 1009, and 1013, the percentage of CTD$^+$ Bmem cells that were class-switched to IgG was 14.8%, 7.3%, and 11.4% respectively (**Figure 2A**). For the CTD$^-$ Bmem cells, 38.2%, 30.1%, and 15.8% of sequences demonstrated class switch (**Figure 2B**). The higher ratio of IgM / IgG expression by CTD$^+$ Bmem cells became apparent late in the present study. PBMCs were therefore obtained from an additional subject (1018) and cultured with polyclonal stimuli to drive differentiation of Bmem cells and detect CTD-specific IgG as well as IgM-secreting cells by ELISPOT (**Figure S3**). In those analyses, CTD$^+$ Bmem cells were dominated by IgM rather than IgG. In contrast, total Bmem cells (representing the CTD$^+$ and CTD$^-$ population) had large frequencies of IgM- as well as IgG-secreting cells.

The IgG subclass distribution was analyzed for CTD$^+$ and CTD$^-$ Bmem cells (**Figure 2A and B**). The relative abundance of each IgG subclass was IgG1>IgG2>IgG3>IgG4 in the CTD$^+$ and the CTD$^-$ Bmem compartments. For each subject, there was no discernable difference in the relative numbers of each IgG subclass between the CTD$^+$ and the CTD$^-$ populations. This data therefore suggests an impediment to class switch amongst CTD$^+$ Bmem cells as compared to Bmem cells of other specificities. However, the conditions determining which subclasses are produced appear to be unaltered between CTD$^+$ and CTD$^-$ Bmem cells.

Similar Ig heavy and light chain variable gene usage in CTD+ and CTD$^-$ Bmem

Repertoire analysis of Bmem cells following specific infections have revealed over-representation of select Ig heavy chain variable (IGHV) gene families [58]. To understand if *C. difficile* skews the IGHV usage in the Bmem cell repertoire, we analyzed the heavy and light chain variable (V)

and joining (J) gene usage for CTD^+ and CTD^- Bmem cells. For the CTD^+ and CTD^- Bmem cells of subjects 1008, 1009, and 1013 (**Figure 3A**), the heavy chain V3 (IGHV3) gene family and specifically the IGHV3-23 gene was the most frequently utilized. A detailed analysis of the V-J gene usage within the IGHV3 gene family confirmed that IGHJ4 was the most prevalent IGHJ gene used by CTD^+ and CTD^- Bmem cells (**Figures 3B, S4A, S4B**). For the light chain it was observed that kappa was most frequently used and the typical ratio of kappa to lambda usage [59] was evident (**Figure 4A and B**). Genes V1 and V3 for kappa and V1, V2 and V3 for lambda were the predominant light chain V genes observed in the study (**Figure 4C and D**). Overall, the V gene usage of the CTD^+ Bmem cells was similar to that observed in CTD^- Bmem cells. Furthermore, the IGHV gene usage was similar in subjects 1008, 1009, and 1013.

Somatic hypermutation in class-switched CTD^+ Bmem

Mutated V(D)J regions are a hallmark of antigen-experienced B cells. While the recombination of V, D and J genes create a large repertoire of B cell receptors, the somatic mutations in V regions add further specificity and allow for affinity maturation. In the present study the IGHV sequences from subjects 1008, 1009, and 1013 were compared to germline sequences to measure the frequency of somatic hypermutation in the V region (**Figure 5**). As expected, the class-switched sequences (IgA and IgG) from both CTD^+ and CTD^- Bmem had higher frequencies of mutations than the IgM^+ sequences. This was the case for replacement mutations that caused amino acid changes and silent mutations that did not cause amino acid changes. However, IgM sequences also had replacement mutations. Furthermore, the complementarity determining regions (CDRs) of the class-switched sequences from the CTD^+ and CTD^- Bmem cells were more frequently mutated than the framework regions (FR) (*data not shown*). CDRs accumulate more replacement mutations than FRs allowing CDRs to be more plastic and antigen-responsive than the FRs that are tasked with maintaining Ab structure [60, 61]. These findings indicated that the CTD^+ Bmem-encoded Abs were not likely to be deficient in

affinity maturation and that some degree of affinity maturation was evident in the IgM compartment.

Similar characteristics of IgG1-switched CTD$^+$ and CTD$^-$ Bmem

Anti-TcdB IgG is the best known correlate of protection against CDI and recurrence [37, 42-45]. IgG1 was the predominant IgG subclass observed amongst IgG$^+$, CTD$^+$ Bmem cells and was analyzed in further detail (**Figure 6**). For all 3 subjects, the VH3 was the most utilized IGHV gene family for IgG1 sequences from CTD$^+$ and CTD$^-$ Bmem (**Figure 6, top**). VH1 and VH4 were the next most frequently used genes. Bmem-encoded Ab were characterized by mutated sequences and the number of IgG1 sequences that had 0 to 50 replacement mutations in their V region was analyzed (**Figure 6, middle**). A majority of the sequences had 11 to 20 replacement mutations in their IGHV regions (consisting of the FR1, FR2, FR3, CDR1 and CDR2 combined). Most of those replacement mutations were in the CDR1 and CDR2 regions (*data not shown*).

Addition and deletion of nucleotides during V(D)J recombination renders the antigen-binding CDR3 loop heterogeneous [62]. Therefore the range of CDR3 amino acid length in the IgG1 sequences of CTD$^+$ and CTD$^-$ Bmem cells was determined. More than 50% of the sequences had CDR3 lengths in the 10-20 amino acid range (**Figure 6, bottom**). Up to 4% had CDR3 lengths of less than 10 amino acids. Only 9-10% IgG1 sequences from the CTD$^-$ subset of all 3 individuals had CDR3 lengths of >20 amino acids. Sequences with CDR3 lengths of >20 amino acids in the CTD$^+$ subset had frequencies of 15% in subject 1008, 21% in 1009 and 9% in 1013. The CTD$^+$ IgG1 sequences in the present study therefore displayed features characteristic of an antigen-experienced repertoire.

Clonal expansion of CTD-specific IgM antibody

The human Bmem compartment is characterized by a high degree of clonal diversity [63]. The clonal families observed in class-switched and non-class-switched CTD^+ and CTD^- Bmem cells from subjects 1008, 1009 and 1013 were therefore analyzed. A majority of the CTD^+ and CTD^- Bmem populations were polyclonal, containing sequences unique within the cell sample analyzed (**Figure 7**). IgM^+ Bmem cells demonstrated several expanded clones. One CTD^+ Bmem clone from subject 1009 had 11 members, while a CTD^- Bmem clone from subject 1013 had 37 members (**Figure 7**).

Class-switched Bmem cells largely consisted of unique clones. All IgA^+ clones were unique except for one clone with 2 members (in CTD^+ Bmem of subjects 1008 and 1009). The IgG^+ clones in CTD^+ Bmem from subjects 1008 and 1009 were unique. Subject 1013 had one IgA^+ clone with 4 members and one IgG^+ clone with 2 members. Furthermore, clones identified from each subject were unique to that individual.

The CTD^- Bmem cells from the 3 subjects demonstrated limited clonal expansion in the IgA^+ Bmem compartment (ranging from 38 clones with 2 members to 1 clone with 7 members). Similarly in the IgG^+ Bmem compartment there was a range of 52 clones with 2 members to 1 clone with 4 members (*data not shown*).

While there was evidence of clonal expansion in CTD^+ Bmem cells, the expansion was largely restricted to a few IgM^+ clones suggesting that CDI may result in a Bmem compartment composed of several unique clones.

Validation of sequencing and analytical strategy using Bmem cells from a healthy control

Validation of the barcoding, sequencing and analytical methods utilized in this study was provided by analyzing total Bmem cells from a healthy control (#1007) (**Figures S5 and S6**). Enriched B cells were harvested and $CD3^-$, $CD19^+$, $CD20^+$, $CD27^+$, $CD38^-$, IgM^+ and $CD3^-$, $CD19^+$, $CD20^+$, $CD27^+$, $CD38^-$, IgM^- Bmem cells were sorted for heavy chain V, diversity (D) and J and light chain V and J repertoire analysis (**Figure S5A**). The healthy IgG subclass

distribution (**Figure S5B**), the V region usage (**Figure S5C**), and the mutation frequency in IgA, IgG, and IgM (**Figure S5D**) were as expected. Further analysis of the mutation frequency in $IgG1^+$ B_{mem} cells (**Figure S6A**), the CDR3 length (**Figure S6B**), and the clonality of the IgM, IgG, and IgA compartments (**Figure S6C**) were also as expected. These features were characteristic of a B_{mem} compartment and served to provide validation for the methods described in analysis of the B_{mem} repertoire from experimental subjects.

Characteristics and functional capacity of fully-human full length anti-CTD antibodies

The best known correlate of protection against primary and recurrent CDI is TcdB-neutralizing IgG of potentially high affinity [37, 42-45, 50, 51]. Experiments were therefore performed to test the antigen binding and functional activity of the IgG1 sequences that were observed in the CTD^+ B_{mem} compartment. Several mAbs were generated from the IgG1 sequences obtained from subjects 1008, 1009 and 1013 respectively. The sequences were selected to represent the VH gene usage, range of CDR3 lengths, and numbers of mutations in the CTD^+, $IgG1^+$ B_{mem} sequences (**Table S2)**. The mAbs were tested for antigen binding and affinity (**Figure 8 and 9**). Of the mAbs generated, 24/49 bound by ELISA to CTD from TcdB1 and 22/49 mAbs bound to CTD from TcdB2 (**Figure 8**). One of the six mAbs (mAb 1009_17) tested bound both TcdB1-CTD and TcdB2-CTD with a less than nanomolar affinity (**Figure 9**). Mab 1009_17 bound TcdB1-CTD with Kd = 0.37 ± 0.14 nM and TcdB2-CTD with Kd = 0.108 ± 0.02 nM. Saturated binding could not be achieved for all mAbs consistent with low to moderate affinity and are designated in the figure as approximate (~) values.

The B_{mem}-encoded mAbs from the 3 subjects were then tested for their ability to neutralize *in vitro* intoxication of CHO cells by TcdB1 and TcdB2 (**Figure 10**). The mAbs from 1008, 1009 and 1013 tested individually or in a variety of combinations were unable to neutralize TcdB1 activity *in vitro*. However, mAb 1009_17 was able neutralize TcdB2 activity *in vitro* resulting in ~60% CHO cell viability (**Figure 10A and C**).

CTD$^+$, IgG1$^+$ Bmem cells lacked clonal expansion and encoded mAbs with limited toxin-neutralizing capacity. We therefore selected sequences from the clonally expanded IgM$^+$, CTD$^+$ Bmem cells of subjects 1008, 1009, and 1013 (**Table S2**). The IgM V(D)J regions were expressed as IgG1 mAbs to control for differences between IgM and IgG1 constant regions. The IgM-V(D)J / IgG1 mAbs were then tested for antigen binding and toxin neutralization activity *in vitro* (**Figure S7**). Only 2/8 mAbs generated showed binding to TcdB1-CTD by ELISA. None of the mAbs demonstrated TcdB1 neutralization *in vitro*.

Plasma obtained from subjects 1008 and 1013 but not 1009 was able to neutralize both TcdB1 and TcdB2 *in vitro*. To confirm that the IgG in the plasma was primarily responsible for the neutralization, we depleted IgG from the plasma of subjects 1008 and 1013 and observed that the samples lost their capacity to neutralize toxin *in vitro* (**Figure 10B and D**). CDI therefore resulted in generation of a toxin-specific plasma cell-derived polyclonal Ab pool containing sufficient amounts of neutralizing Ab for *in vitro* toxin neutralization.

DISCUSSION

Typically, the host immune system establishes 'memory' to a primary infection resulting in a rapid and effective response upon re-exposure to a pathogen. A recent study from our laboratory revealed that an initial infection of mice with *C. difficile* spores did not induce a CTD/TcdB-specific B_{mem} response or protect from pathology associated with repeat infection [64]. This is consistent with another study from our laboratory where human subjects with a history of CDI demonstrated poor differentiation of CTD-specific B_{mem} cells into new plasmablasts following polyclonal stimulation [33]. Recurrent CDI could therefore result from an inadequate B_{mem} cell response. Studies with human subjects have shown that neutralizing serum IgG specific for *C. difficile* TcdB is associated with protection against primary and recurrent infections [42, 43]. However, the human TcdB-specific B_{mem} repertoire and whether it encodes TcdB-neutralizing Ab has not been evaluated. This is the first study, to the best of our knowledge that determined the repertoire and function of CTD^+ B_{mem} from individuals with a self-reported history of CDI.

Antigen-specific B_{mem} cells occur in low frequencies in human PBMCs. We therefore isolated TcdB1-CTD^+ and -CTD^- B_{mem} cells, single-cell barcoded them and then examined their Ig genes by deep sequencing. Surprisingly, the CTD^+ B_{mem} cells had a much lower proportion of class-switched Abs than the CTD^- B_{mem} cell population. These IgM^+ sequences from the CTD^+ B_{mem} cells had undergone somatic hypermutation as evidenced by changes compared to germline sequences. The presence of mutations in the IgM sequences in conjunction with our cell-sorting strategy which excluded $CD38^+$ cells confirmed that these were not natural Ab-secreting cells [65]. We observed a much higher frequency of IgM^+ rather than IgG^+, CTD^+ B_{mem} cells in our ELISPOT assays as well. These findings are consistent with our observation of limited class switch and IgM dominance in our recently published study using a mouse model of *C. difficile* recurrence [64].

IgM$^+$ Bmem cells have been observed in human PBMCs in response to T-independent antigens such as polysaccharides [66] and malaria infection [67]. To the best of our knowledge this is the first report demonstrating a predominantly IgM$^+$ Bmem cell compartment following CDI. Several of the CTD$^+$ IgM sequences were clonally related forming clones with up to 11 members. Recent studies have described IgM that can neutralize Chikungunya virus early in infection [68], that can block HIV-transmission in cervico-vaginal tissues [69], and that can afford protection against Influenza [70]. However, we observed that the CTD$^+$, IgM$^+$ Bmem cell-encoded Ab did not neutralize TcdB1-CTD. We did not anticipate Bmem-encoded CTD-specific IgM to play a role in neutralizing toxin since there are several studies that have demonstrated IgG to be the best correlate of protection to CDI [37, 42-45]. Furthermore, the IgG-depleted plasma samples in our study were unable to neutralize toxin *in vitro* emphasizing the role of IgG in preventing recurrent CDI.

Analysis of IGHV gene usage in adults with rotavirus-experienced B cells show bias in their use of the VH1 and VH4 genes [71]. VH analysis in B cells from individuals with autoimmune disease have demonstrated VH4 and VH5 biases in SLE and VH3 bias in myasthenia gravis [72]. To understand if CDI resulted in a biased VH repertoire, we analyzed the VH gene usage of CTD$^+$ and CTD$^-$ Bmem cells and found no differences between them. Consistent with previous studies involving healthy individuals, we observed that the V3 and J4 gene families dominated the heavy chain repertoire [73-75]. The IGHV regions from class-switched CTD$^+$ Bmem cells, from CTD$^+$, IgM$^+$ Bmem cells, and from CTD$^-$ Bmem cells had undergone somatic hypermutation. This demonstrates that the affinity maturation process in patients was intact.

The ratio of replacement to silent mutations in the CDR1 and 2 regions of several class-switched sequences from CTD$^+$ Bmem cells was >2.9 suggesting antigenic selection of those clones [76]. Although IgG only accounted for about 10% of the CTD$^+$ Bmem cells, the subclass

distribution was similar to that observed for the CTD^- Bmem cells with IgG1 accounting for a majority of the IgG^+ sequences. As is typical for class-switched Bmem cells, the IgG1 sequences had CDR3 lengths of up to 20 amino acids and an increased VH1 usage as compared to memory IgM sequences [77]. Overall, these findings suggested that the CTD^+ Bmem cells encoded a repertoire that was theoretically capable of neutralizing TcdB. For this reason, several IgG1 mAbs were generated from the sequences obtained from each subject to test their binding specificity to and their affinity for CTD from TcdB1 and TcdB2. We also tested the ability of these IgG1 mAbs to neutralize TcdB1 and TcdB2 in an *in vitro* CHO cell viability assay. While almost fifty percent of the 49 IgG1 mAbs generated bound CTD by ELISA only one mAb (1009_17) bound with high affinity (*Kd* = 0.108 ± 0.02 nM) and neutralized TcdB2 to prevent CHO cell killing *in vitro*. This supports the possibility that CTD-specific Bmem cells encode mostly low-affinity Ab incapable of toxin neutralization. Bezlotoxumab, a TcdB-targeting human mAb FDA-approved only for prevention of recurrent CDI [78, 79] binds high affinity sites in the full-length TcdB1 with a *Kd* of 19 ± 5 pM [49]. This *Kd* is 19-fold greater than the *Kd* with which the highest affinity mAb expressed in this study binds TcdB1 (1009_17; *Kd*= 0.37 ± 0.14 nM). While the CTD binding site for bezlotoxumab has been characterized [49], the specific binding sites for the mAbs generated in this study remain to be identified.

It should be noted that although CTD-binding and toxin-neutralizing Bmem-cell encoded mAbs were generated for this study, the question remains as to whether these Bmem cells have the capacity to differentiate in response to CDI and express Abs *in vivo*. This is attested by the inability of plasma from subject 1009 to neutralize toxin *in vitro* although their Bmem compartment encoded a toxin-neutralizing mAb. In our recent murine studies, CDI resulted in a poor expansion of $PD\text{-}1^{hi}$, $CXCR5^+$ follicular helper T cells (Tfh) [64]. This lack of T cell-help could limit Bmem cell expansion and differentiation into Ab-secreting plasma cells. The role of

Tfh in this study could not be explored since the subject samples were obtained several months after infection.

It is also possible that CTD-specific Bmem cells encode low-affinity Ab incapable of toxin neutralization. This is supported by the mostly low to moderate affinity mAbs produced from the CTD-specific Bmem cell pool in the present study and the observation that the only mAb (1009_17) that bound TcdB2-CTD with high affinity also successfully neutralized TcdB2 in an *in vitro* viability assay.

Differences in disease severity could also influence the Bmem response. Although 1008, 1009 and1013 self-reported a single infection in the five years before recruitment into this study, they all reported being symptomatic. 1008 and 1013 reported receiving medical treatment and only 1013 reported being hospitalized due to CDI. Due to the lack of complete medical history, we cannot comment on the influence of disease severity on the humoral response in our cohort. An alternative hypothesis is that Bmem-encoding neutralizing Ab may only develop after several recurrent infections at which point the individual may not benefit from those Ab due to the extensive gut damage from previous infections. Comparing the Bmem cell repertoires in individuals following recurrent and non-recurrent infections may allow testing of this hypothesis, but the high mortality rate in individuals with recurrent disease may preclude a larger study.

It is very likely the study participants could have been infected with a *C. difficile* strain other than the historical VPI 10463 strain and therefore their Bmem-encoded Abs did not neutralize TcdB1. While Abs produced in response to TcdB2 from the hyper-virulent NAP1/027/BI strain cross-react with TcdB1 from the historical strain, the cross-neutralization between strains is limited [28, 33, 80]. This was confirmed in our analysis where one mAb from subject 1009 bound CTD from both TcdB1 and TcdB2 but only neutralized TcdB2 *in vitro*. In this study we tested the CTD-specific Bmem response, but the response to TcdB (whole toxin) could arguably be broader. However, we observed that the plasma anti-TcdB1-CTD IgG response

386 was very similar to the anti-TcdB1 IgG response and the same plasma samples had
387 background level reactivity to a recombinant TcdB1 glucosyltransferase domain (*data not*
388 *shown*). These findings combined with previously published literature indicating the antigenicity
389 and neutralizing capacity of CTD [33, 55, 56] indicate a predominantly CTD-specific Bmem
390 repertoire.

391 The lack of TcdB1 neutralization by the Bmem-encoded mAbs appeared to contrast with
392 that of plasma samples from subjects 1008 and 1013 which neutralized toxin in an IgG-
393 dependent manner. A discrepancy between plasma antibody titers and circulating Bmem cell
394 frequency and function has been documented for *C. difficile* and other bacterial toxins and has
395 been proposed as a feature of the host humoral response to bacterial toxins [54, 81]. Although,
396 this study was not designed to investigate differences between Bmem and plasma cell-derived
397 Ab, there could be several explanations for this observation. Arguably, the simplest explanation
398 is that only a small proportion of plasma cell-derived Abs are toxin-neutralizing, but sufficient
399 neutralizing Ab had accumulated in the sera to be functional in the *in vitro* assay. Similarly, very
400 few Bmem cells may encode neutralizing Ab, explaining why only one mAb of 49 was
401 neutralizing. The TcdB-neutralizing Ab observed in plasma samples is likely composed of
402 numerous-fine specificities targeting several epitopes on the toxin allowing more efficient toxin
403 neutralization. Plasma from subjects 1008 and 1013 neutralized both TcdB1 and TcdB2 *in vitro*,
404 possibly alluding to a requirement for combating CDI with Abs of multiple specificities. In this
405 study it was observed that several cocktails of three different Bmem cell-derived anti-CTD mAbs
406 failed to neutralize toxin *in vitro*.

407 Finally, a caveat to extrapolating from *in vitro* toxin neutralization studies is that they may
408 not accurately predict *in vivo* protection [82, 83]. Toxin concentration and availability of
409 neutralizing Ab in the gut lumen as well as rate of toxin clearance are likely to influence disease
410 progression, severity and treatment of CDI [26, 84, 85].

411 Several vaccine candidates to prevent CDI are in clinical trials and while they show
412 promise, their efficacy remains to be determined [86]. Our study highlights the necessity of
413 considering the basic immune response to this infection as well as designing and testing new
414 vaccines. In an animal model, immunization with CTD followed by CDI did not generate a recall
415 response [64] and the animals were protected due to the Ab secreted by plasma cells generated
416 in response to prior immunization. Similarly, this study demonstrated that CDI did not establish
417 an efficient memory response in humans. This implies a requirement for repeated vaccinations
418 to sustain an adequate protective response to future infections.

419 Further studies comparing B_{mem} cell repertoires in larger cohorts of individuals with
420 single-episodes of CDI or recurrent CDI will allow a deeper understanding of how *C. difficile*
421 impacts the host humoral immune response. Comparing the plasma cell-derived Ab repertoire
422 with that of the B_{mem}-derived Ab repertoire may provide further insights. Finally, the immune
423 response to *C. difficile* antigens other than the toxin need to be evaluated.

METHODS

Human subjects' eligibility, recruitment and selection. The present study was designed to identify individuals with a history of CDI and determine their Bmem-encoded Ab repertoire. To achieve this goal, blood samples were collected from males and females who either had CDI within the past 5 years (subjects) or had no known history of CDI (controls). Individuals aged 20 - 85 and asymptomatic at the time of the blood draw were eligible for the study. Individuals with a history of major health issues including autoimmune disease, cancer, cardiovascular disease, or ongoing infectious disease (including HIV) were excluded from the study. Individuals who were presently unhealthy, had been vaccinated within the past month, or weighed less than 110 pounds were also excluded. Subjects included in this study self-reported receiving a laboratory-based diagnosis for CDI and reported no complications from CDI. Subjects 1008 and 1009 self-reported single episodes of CDI at the time of recruitment. Subject 1013 self-reported two episodes three years apart with the first episode occurring almost six years before recruitment in this study and was hospitalized due to the second episode. Since the second episode for subject 1013 did not occur within 12 weeks of the first infection, it did not meet the criteria for recurrent CDI [51]. Blood samples were analyzed to determine if individuals had a detectable population of *C. difficile* toxin B-specific (CTD fragment of TcdB) Bmem cells. Subjects 1008, 1009 and 1013 had demonstrable CTD-specific Bmem cells in peripheral blood as detailed in the results and were available for a second visit to provide sample for repertoire analysis. Repertoire analysis was therefore performed on CTD^+ and CTD^- Bmem cells from subjects 1008, 1009 and 1013. To validate our isolation, sequencing and analytical methods we isolated total Bmem cells from a healthy control (1007) for repertoire analysis. Details for individuals included in this study are presented in Supplemental Table 1.

Sample procurement, PBMC preparation, and B cell enrichment. Peripheral venous blood was drawn from healthy subjects into vacuum tubes containing acid citrate dextrose (BD Biosciences, San Jose, CA). Samples were centrifuged for 15 min at 400 *rcf* at room temperature to collect plasma. Packed blood was mixed with an equal volume of 1 x PBS, layered onto 15 ml of lymphocyte separation medium, known as LSM (Lonza, Allendale, NJ) and centrifuged at 800 *rcf* (no brake) for 30 min at room temperature. PBMCs collected using a pipette were washed with PBS and re-suspended in PBS containing 2% v/v fetal calf serum (FCS). PBMCs were used for initial flow cytometry analysis. The RosetteSep™ Human B cell enrichment cocktail (Stemcell, Cambridge, MA) was used for B cell enrichment according to the manufacturer's instructions. Briefly, whole blood was mixed with RosetteSep™ cocktail (50 µl/ml of blood sample) and allowed to incubate for 20 min at room temperature. The sample was then diluted by adding an equal volume of PBS / 2% v/v FCS. After mixing gently, the diluted sample was layered on to LSM and centrifuged at 1200 *rcf* (no brake) for 20 min at room temperature. The enriched B cell population was collected from the top of the LSM layer, washed in PBS, and re-suspended in PBS / 2% v/v FCS. The enriched B cell samples were used as starting material for B_{mem} cell labeling and sorting.

Flow cytometry and cell sorting

Where indicated PBMCs or enriched B cells were incubated with flurochrome-conjugated mAb against cell surface proteins at 4°C for 30 min, before washing 3 times with PBS containing 2% FCS. The following anti-human mAbs were used: PE-Alexa Fluor 610 CD19 (clone: SJ25C-1), Pacific Orange CD20 (clone: HI47) APC-Alexa Fluor 750 CD27 (clone CLB-27/1) and APC-Cy5.5 CD38 (clone: HIT2) from Invitrogen (Frederick ,MD), PE-Cy7 CD3 (clone: UCHT1), APC IgG (clone:G18-145) from BD Biosciences (San Jose, CA) and PE-IgM (clone:UHB) from SouthernBiotech (Birmingham, AL). Data were collected using a FACSAria™ III instrument and

analyzed using FlowJo_V10 software (BD Biosciences). For Bmem cell isolation, enriched B cells were first selected for size and granularity using FSC/SSC followed by gating for singlets. The $CD3^-/CD20^+/CD19^+/CD27^+/CD38^-$ cells were then selected to obtain Bmem cells. $CD20^+$, $CD27^+$, $CD43^+$, $CD70^-$, $CD38^+$, $CD5^+$ cells were therefore not collected during sorting [65]. Where indicated, cells were counterstained with Alexa488-CTD to facilitate simultaneous sorting of CTD^+ and CTD^- Bmem cells. B cell receptor blocking was achieved by adding 20 µl goat anti-human IgG, IgM and IgA (H&L) from Genway biotech (San Diego, CA) per 2 x 10^6 PBMCs. After a 30 min incubation at 4°C the samples are washed once with PBS containing 2% FCS before adding Alexa488-CTD.

Expression and purification of TcdB and CTD and CTD labeling. TcdB from strain VPI-10463 and NAP1/BI/027 was purified using established methods [28, 87]. The CTD-encoding region of the tcdb gene was codon-optimized and cloned into the pET15b plasmid (Genscript, Piscataway, NJ) as described previously [33]. Briefly, the VPI-10463 and NAP1/BI/027 CTD genes were amplified using primers 5′-GATCATATGCTGTATGTGGGTAACCG-3′ and 5′-AACGGATCCTTATTCGCTAATAACCA-3′ and restriction sites BamHI and NdeI were included for cloning into pET15b. VPI-10463 TcdB is referred to as TcdB1 and NAP1/BI/027 TcdB is referred to as TcdB2. VPI-10463 CTD (TcdB1 amino acids 1651–2366) and NAP1/BI/027 CTD (TcdB2 amino acids 1651–2366) were expressed in *Escherichia coli* BL21 star DE3 (Invitrogen, Frederick, MD) and purified by $Ni2^+$ affinity chromatography (HisTrap; GE Life Sciences, Marlborough, MA). The holotoxin and CTD are expressed and purified using the same method and the structure of the CTD obtained maintains the same structure as the holotoxin [49]. Mouse splenocytes were cultured with the CTD preparation which failed to cause polyclonal B cell expansion and IgM secretion, as is expected for LPS, thus confirming sufficient LPS removal during purification. An Alexa Fluor® 488 protein labeling kit (Invitrogen, Frederick, MD) was used to label CTD from TcdB1 according to the manufacturer's instructions.

Barcoding and library construction. Sorted CTD^+ and CTD^- B_{mem} cells were processed using the Chromium Single Cell V(D)J Enrichment Kit for human B cells in conjunction with a Chromium controller. This was performed according to the manufacturer's instructions (10X Genomics, Pleasanton, CA) and as described previously [88]. Briefly, each cell was partitioned along with a single barcoded Gel Bead into an individual Gel bead-in-emulsion (GEM). Once the Gel Bead dissolved and the cell was lysed, a reverse transcription reaction allowed the cell to be individually and uniquely barcoded. The barcoded cDNA was then amplified with primers specific to Ig constant regions resulting in targeted enrichment of the V(D)J. The V(D)J enrichment kit included all reagents and primers for PCR amplification of the full length variable and constant regions. This process resulted in a library of full length Ig genes ready for Next Generation Sequencing.

Next Generation Sequencing. The amplified transcripts were sequenced using a NovaSeq S1 System (Illumina, San Diego, CA) by the Oklahoma Medical Research Foundation Clinical Genomics Center. Libraries were sequenced to a depth of 200 million paired reads. The raw output files were processed using Cell Ranger™ 3.0.2 software (10X Genomics) to generate FASTA files for further analysis. For the CTD^+ B_{mem} cells this resulted in 2262, 4394, and 1826 annotated heavy and light chain sequences for subjects 1008, 1009 and 1013 respectively. For the CTD^- B_{mem} cells this resulted in 16684, 16009, and 15868 annotated sequences for subjects 1008, 1009 and 1013 respectively. These sequences were further curated for full-length, productive sequences that had a single heavy and light chain pair. This curation resulted in 506, 948 and 527 CTD^+ B_{mem} sequences and 4443, 4612 and 3845 CTD^- B_{mem} sequences used in this study for subjects 1008, 1009 and 1013 respectively. Difference in frequency of sequences between 1009 and other subjects was less than 2-fold for both CTD^+ and CTD^- B_{mem} cells allowing appropriate comparisons.

RNA-seq data analysis. The FASTA files were uploaded to the IMGT HighVQuest website (http://imgt.org/HighV-QUEST/home.action). Data from IMGT HighVQuest was parsed in RStudio [RStudio Team (2019). RStudio: Integrated Development for R. RStudio, Inc., Boston, MA URL http://www.rstudio.com/)] using MakeDb.py from Change-O[89]. This data was then filtered to keep barcodes associated with sequences that were functional, full-length and had only one heavy chain and light chain pair. Clones were defined and germlines assigned with DefineClones.py and CreateGermlines.py, respectively from Change-O using the hamming distance algorithm. To assign clonally–related sequences, a clustering threshold of 85% (CDR3 sequence similarity) was determined with distToNearest() and findThreshold(). Mutations in the heavy chain V regions were calculated using observedMutations() from the SHazaM R package [89].

Human monoclonal antibody synthesis. Genes for mAb generation were selected from the IgG1 sequences from CTD^+ B_{mem} cells (Supplemental Table 2). To limit selection bias, sequences that spanned various heavy chain CDR3 lengths, numbers of V region mutations, and V region usage were included. The mAbs were generated using a previously published method [90] with the exception of using sequences generated using 10X Genomics technology rather than single-cell RT-PCR. To express mAbs from CTD^+, IgM^+ B_{mem} cells from each subject, we selected sequences belonging to clonal families with several members (1008 - 4 members; 1009 - 8, 9 and 11 members and 1013 – 6 members). The heavy chain V region from these sequences were expressed with an IgG1 heavy chain constant region. After deep sequencing heavy and light chain genes were synthesized by IDT (Integrated DNA Technologies, San Diego, CA). These genes were then cloned into separate heavy and light chain (kappa or lambda as appropriate) vectors and transformed using DH5α competent cells (Invitrogen, Frederick, MD). Four colonies were picked from the transformation for mini-prep

followed by sequencing. The sequences from each of the colonies was matched to the consensus and the best match was moved forward to maxi-scale preparation. Human kidney epithelial cells (HEK293 cell line; ATCC, Manassas, VA) were transiently co-transfected with heavy and light chain vectors using polyethylenimine and the cells were allowed to produce Ab over 5 days. Pierce™ Protein A agarose beads (Thermo Fisher Scientific, Waltham, MA) were used to purify the mAb from the cell culture supernatant. The mAbs were then analyzed for concentration, specificity and biological activity.

Enzyme Linked Immunosorbent Assay

Maxisorp (ThermoFisher) plates were coated with 100 µl/well of CTD (10 µg/mL) diluted in carbonate coating buffer and incubated at 4^{o}C overnight. After washing with PBS / 0.05%Tween 20, plates were blocked with 200 µl/well PBS / 0.05%Tween 20/1%BSA (blocking buffer) for 2 hr at room temperature. After washing the plates, 100 µl/well of mAbs diluted 10 µg/mL in blocking buffer were added and allowed to incubate for 2 hr at room temperature. After four washes, HRP-anti human IgG (Jackson, 1:2500 in blocking buffer) was added to plates and incubated for 1 hr at room temperature. ABTS was added to develop the plates and stop buffer (10% SDS w/v ddH_2O) was added to stop the reaction after 5 min. OD was measured at 405 nm. For some of the mAbs individual ELISA curves generated from a series of 16 two-fold dilutions of the Ab starting at 10 µg/mL were applied to a curve fitting analysis to calculate Ab affinities (*K*d) as described [91].

***In vitro* Neutralization assay**

CHO cells were re-suspended at 1 x 10^5 cells / mL in F-12K media with L-glutamine and 10% heat-inactivated FCS and 100 µL of the cell suspension was seeded into each well of the 96-well plates and cultured overnight (5% CO2, 37°C). Human mAbs and plasma samples were diluted to 10 µg/mL and 1/100 respectively in medium containing TcdB1 or TcdB2 at a final

concentration of 0.23 nM and 0.25 nM respectively and incubated for 30 mins at 37ºC. A positive control serum was obtained from rabbits immunized and boosted with 0.1 mg of the CTD fraction of *C. difficile* VPI 10463 ribotype as described previously [57]. IgG depletion from plasma samples was achieved using Albumin and IgG Depletion SpinTrap columns (GE Life sciences, Marlborough, MA) prepacked with agarose beads covalently bound to anti-HSA and Protein G. The toxin concentration was calibrated to cause 80% CHO cell death. Medium from 24 hr old cultures was removed and replaced with the Ab/plasma-toxin-medium mixture. Plates were cultured for 24 hr before addition of 100 µL/well of media containing 10% Cell Counting kit-8 (CCK-8) reagent (Sigma, St. Louis, MO) and an additional 2 hr of incubation. A450 was then measured, and percent viability was calculated as follows: [A450 of treated (sample-toxin) cells/A450 of untreated (no toxin) cells] × 100.

Statistics

GraphPad Prism (GraphPad Software, Inc., La Jolla, CA) was used to generate binding curves and calculate equilibrium dissociation constants (*K*d) to report mAb affinity. For multiple comparisons Kruskal-Wallis with Dunn's post-test correction was used as indicated. An unpaired t test with Welch's correction was used to compare two groups. p values of <0.05 were considered significant.

Study Approval

Written informed consent was given by study participants. The human subject studies were approved by the OUHSC Institutional Review Board (Protocol #8158) and were performed in accordance with the ethical standards as laid down in the 1964 Declaration of Helsinki and its later amendments.

Dataset availability

Sequences are submitted to the NCBI Sequence Read Archive (SRA) and the project is registered with the BioProject database under SRA accession: PRJNA601978 (http://www.ncbi.nlm.nih.gov/bioproject/601978). The accession numbers for the data are: SAMN13878386 (1007), SAMN13878387 (1008), SAMN13878388 (1009) and SAMN13878389 (1013).

Author Contributions

H.S. designed and performed the experiments, analyzed data and wrote the manuscript. M.L. devised the project, analyzed data, and wrote the manuscript. E.S performed bioinformatics analysis and curated the data. K.S. generated and quality control checked the mAbs, analyzed data and edited the manuscript. J.L provided critical reagents and assisted with neutralization experiments. J.B. provided critical reagents, reviewed data, and edited the manuscript. J.J. assisted with subject recruitment, reviewed data, and edited the manuscript.

Acknowledgements and Funding

Brittany Karfonta and Katlyn Beecken at the Oklahoma Shared Clinical and Translational Resources (OSCTR) supported by National Institutes of Health [(NIH) award number U54GM104938] provided assistance with patient recruitment and sample collection. Assistance with data analysis was provided by the Bioinformatics core (supported by NIH award number P20GM10344). The content is solely the responsibility of the authors and does not necessarily represent the official views of the NIH. The experimental work described in this manuscript was supported by a Team Science research award from the Presbyterian Health Foundation of Oklahoma City. We acknowledge the Flow cytometry core, Genomics Core and the Human Ab Core at OMRF for their assistance in cell sorting, sequencing and Ab generation respectively. The authors thank Dr. Willard Freeman (OMRF) for access to the Chromium controller and Drs. Carol Webb and David Dyer (OUHSC) and Jonathan Wren (OMRF) for helpful discussions.

REFERENCES

1. Lessa, F.C., et al., *Burden of Clostridium difficile infection in the United States.* N Engl J Med, 2015. **372**(24): p. 2369-70.
2. Barbut, F., et al., *Prospective study of Clostridium difficile infections in Europe with phenotypic and genotypic characterisation of the isolates.* Clin Microbiol Infect, 2007. **13**(11): p. 1048-57.
3. Bauer, M.P., et al., *Clostridium difficile infection in Europe: a hospital-based survey.* Lancet, 2011. **377**(9759): p. 63-73.
4. Davies, K.A., et al., *Underdiagnosis of Clostridium difficile across Europe: the European, multicentre, prospective, biannual, point-prevalence study of Clostridium difficile infection in hospitalised patients with diarrhoea (EUCLID).* Lancet Infect Dis, 2014. **14**(12): p. 1208-19.
5. Borren, N.Z., et al., *The emergence of Clostridium difficile infection in Asia: A systematic review and meta-analysis of incidence and impact.* PLoS One, 2017. **12**(5): p. e0176797.
6. George, R.H., et al., *Identification of Clostridium difficile as a cause of pseudomembranous colitis.* Br Med J, 1978. **1**(6114): p. 695.
7. Bartlett, J.G., et al., *Role of Clostridium difficile in antibiotic-associated pseudomembranous colitis.* Gastroenterology, 1978. **75**(5): p. 778-82.
8. Larson, H.E., et al., *Clostridium difficile and the aetiology of pseudomembranous colitis.* Lancet, 1978. **1**(8073): p. 1063-6.
9. Rexroth, G., *[Toxic megacolon in pseudomembranous colitis. Complicated course of antibiotic-induced Clostridium difficile colitis].* Fortschr Med, 1993. **111**(13): p. 219-23.
10. Dobson, G., C. Hickey, and J. Trinder, *Clostridium difficile colitis causing toxic megacolon, severe sepsis and multiple organ dysfunction syndrome.* Intensive Care Med, 2003. **29**(6): p. 1030.
11. Elliott, B., et al., *Clostridium difficile-associated diarrhoea.* Intern Med J, 2007. **37**(8): p. 561-8.
12. Karas, J.A., D.A. Enoch, and S.H. Aliyu, *A review of mortality due to Clostridium difficile infection.* J Infect, 2010. **61**(1): p. 1-8.
13. Sakurai, T., et al., *Liver abscess caused by Clostridium difficile.* Scand J Infect Dis, 2001. **33**(1): p. 69-70.
14. Tsourous, G.I., et al., *A case of pseudomembranous colitis presenting with massive ascites.* Eur J Intern Med, 2007. **18**(4): p. 328-30.
15. Boaz, A., et al., *Pseudomembranous colitis: report of a severe case with unusual clinical signs in a young nurse.* Dis Colon Rectum, 2000. **43**(2): p. 264-6.
16. Jacob, S.S., et al., *Clostridium difficile and acute respiratory distress syndrome.* Heart Lung, 2004. **33**(4): p. 265-8.
17. Kuehne, S.A., et al., *The role of toxin A and toxin B in Clostridium difficile infection.* Nature, 2010. **467**(7316): p. 711-3.
18. Lyerly, D.M., et al., *Effects of Clostridium difficile toxins given intragastrically to animals.* Infect Immun, 1985. **47**(2): p. 349-52.
19. Lyras, D., et al., *Toxin B is essential for virulence of Clostridium difficile.* Nature, 2009. **458**(7242): p. 1176-9.
20. Just, I., et al., *Glucosylation of Rho proteins by Clostridium difficile toxin B.* Nature, 1995. **375**(6531): p. 500-3.
21. Just, I., et al., *The enterotoxin from Clostridium difficile (ToxA) monoglucosylates the Rho proteins.* J Biol Chem, 1995. **270**(23): p. 13932-6.
22. Yu, H., et al., *Identification of toxemia in patients with Clostridium difficile infection.* PLoS One, 2015. **10**(4): p. e0124235.

23. Drudy, D., S. Fanning, and L. Kyne, *Toxin A-negative, toxin B-positive Clostridium difficile.* Int J Infect Dis, 2007. **11**(1): p. 5-10.
24. Lin, Q., et al., *Toxin A-predominant Pathogenic C. difficile: A Novel Clinical Phenotype.* Clin Infect Dis, 2019.
25. Steele, J., et al., *Piglet models of acute or chronic Clostridium difficile illness.* J Infect Dis, 2010. **201**(3): p. 428-34.
26. Steele, J., et al., *Systemic dissemination of Clostridium difficile toxins A and B is associated with severe, fatal disease in animal models.* J Infect Dis, 2012. **205**(3): p. 384-91.
27. Siarakas, S., E. Damas, and W.G. Murrell, *Is cardiorespiratory failure induced by bacterial toxins the cause of sudden infant death syndrome? Studies with an animal model (the rabbit).* Toxicon, 1995. **33**(5): p. 635-49.
28. Lanis, J.M., S. Barua, and J.D. Ballard, *Variations in TcdB activity and the hypervirulence of emerging strains of Clostridium difficile.* PLoS Pathog, 2010. **6**(8): p. e1001061.
29. Hunt, J.J. and J.D. Ballard, *Variations in virulence and molecular biology among emerging strains of Clostridium difficile.* Microbiol Mol Biol Rev, 2013. **77**(4): p. 567-81.
30. McDonald, L.C., et al., *An epidemic, toxin gene-variant strain of Clostridium difficile.* N Engl J Med, 2005. **353**(23): p. 2433-41.
31. Muto, C.A., et al., *A large outbreak of Clostridium difficile-associated disease with an unexpected proportion of deaths and colectomies at a teaching hospital following increased fluoroquinolone use.* Infect Control Hosp Epidemiol, 2005. **26**(3): p. 273-80.
32. Loo, V.G., et al., *A predominantly clonal multi-institutional outbreak of Clostridium difficile-associated diarrhea with high morbidity and mortality.* N Engl J Med, 2005. **353**(23): p. 2442-9.
33. Devera, T.S., et al., *Memory B Cells Encode Neutralizing Antibody Specific for Toxin B from the Clostridium difficile Strains VPI 10463 and NAP1/BI/027 but with Superior Neutralization of VPI 10463 Toxin B.* Infect Immun, 2016. **84**(1): p. 194-204.
34. Sheitoyan-Pesant, C., et al., *Clinical and Healthcare Burden of Multiple Recurrences of Clostridium difficile Infection.* Clin Infect Dis, 2016. **62**(5): p. 574-580.
35. Drekonja, D.M., et al., *Antimicrobial use and risk for recurrent Clostridium difficile infection.* Am J Med, 2011. **124**(11): p. 1081 e1-7.
36. Louie, T.J., et al., *Effect of age on treatment outcomes in Clostridium difficile infection.* J Am Geriatr Soc, 2013. **61**(2): p. 222-30.
37. Kyne, L., et al., *Association between antibody response to toxin A and protection against recurrent Clostridium difficile diarrhoea.* Lancet, 2001. **357**(9251): p. 189-93.
38. Marsh, J.W., et al., *Association of relapse of Clostridium difficile disease with BI/NAP1/027.* J Clin Microbiol, 2012. **50**(12): p. 4078-82.
39. Petrella, L.A., et al., *Decreased cure and increased recurrence rates for Clostridium difficile infection caused by the epidemic C. difficile BI strain.* Clin Infect Dis, 2012. **55**(3): p. 351-7.
40. Gomez, S., F. Chaves, and M.A. Orellana, *Clinical, epidemiological and microbiological characteristics of relapse and re-infection in Clostridium difficile infection.* Anaerobe, 2017. **48**: p. 147-151.
41. Olsen, M.A., et al., *Recurrent Clostridium difficile infection is associated with increased mortality.* Clin Microbiol Infect, 2015. **21**(2): p. 164-70.
42. Leav, B.A., et al., *Serum anti-toxin B antibody correlates with protection from recurrent Clostridium difficile infection (CDI).* Vaccine, 2010. **28**(4): p. 965-9.
43. Aronsson, B., et al., *Serum antibody response to Clostridium difficile toxins in patients with Clostridium difficile diarrhoea.* Infection, 1985. **13**(3): p. 97-101.
44. Kyne, L., et al., *Asymptomatic carriage of Clostridium difficile and serum levels of IgG antibody against toxin A.* N Engl J Med, 2000. **342**(6): p. 390-7.

45. Gupta, S.B., et al., *Antibodies to Toxin B Are Protective Against Clostridium difficile Infection Recurrence.* Clin Infect Dis, 2016. **63**(6): p. 730-734.
46. Nakamura, S., et al., *Isolation of Clostridium difficile from the feces and the antibody in sera of young and elderly adults.* Microbiol Immunol, 1981. **25**(4): p. 345-51.
47. Haines, C.F., et al., *Clostridium difficile in a HIV-infected cohort: incidence, risk factors, and clinical outcomes.* AIDS, 2013. **27**(17): p. 2799-807.
48. Collini, P.J., et al., *Clostridium difficile infection in HIV-seropositive individuals and transplant recipients.* J Infect, 2012. **64**(2): p. 131-47.
49. Orth, P., et al., *Mechanism of action and epitopes of Clostridium difficile toxin B-neutralizing antibody bezlotoxumab revealed by X-ray crystallography.* J Biol Chem, 2014. **289**(26): p. 18008-21.
50. Lowy, I., et al., *Treatment with monoclonal antibodies against Clostridium difficile toxins.* N Engl J Med, 2010. **362**(3): p. 197-205.
51. Wilcox, M.H., et al., *Bezlotoxumab for Prevention of Recurrent Clostridium difficile Infection.* N Engl J Med, 2017. **376**(4): p. 305-317.
52. Kurosaki, T., K. Kometani, and W. Ise, *Memory B cells.* Nat Rev Immunol, 2015. **15**(3): p. 149-59.
53. Nutt, S.L., et al., *The generation of antibody-secreting plasma cells.* Nat Rev Immunol, 2015. **15**(3): p. 160-71.
54. Monaghan, T.M., et al., *Circulating antibody and memory B-Cell responses to C. difficile toxins A and B in patients with C. difficile-associated diarrhoea, inflammatory bowel disease and cystic fibrosis.* PLoS One, 2013. **8**(9): p. e74452.
55. Torres, J.F. and T.P. Monath, *Antigenicity of amino-acid sequences from Clostridium difficile toxin B.* J Med Microbiol, 1996. **44**(6): p. 464-74.
56. Babcock, G.J., et al., *Human monoclonal antibodies directed against toxins A and B prevent Clostridium difficile-induced mortality in hamsters.* Infect Immun, 2006. **74**(11): p. 6339-47.
57. Lanis, J.M., et al., *Clostridium difficile 027/BI/NAP1 encodes a hypertoxic and antigenically variable form of TcdB.* PLoS Pathog, 2013. **9**(8): p. e1003523.
58. Shah, H.B., et al., *Insights From Analysis of Human Antigen-Specific Memory B Cell Repertoires.* Front Immunol, 2018. **9**: p. 3064.
59. Barandun, S., et al., *Deficiency of kappa- or lambda-type immunoglobulins.* Blood, 1976. **47**(1): p. 79-89.
60. Chang, B. and P. Casali, *The CDR1 sequences of a major proportion of human germline Ig VH genes are inherently susceptible to amino acid replacement.* Immunol Today, 1994. **15**(8): p. 367-73.
61. Rajewsky, K., *Clonal selection and learning in the antibody system.* Nature, 1996. **381**(6585): p. 751-8.
62. Sanz, I., *Multiple mechanisms participate in the generation of diversity of human H chain CDR3 regions.* J Immunol, 1991. **147**(5): p. 1720-9.
63. Budeus, B., et al., *Complexity of the human memory B-cell compartment is determined by the versatility of clonal diversification in germinal centers.* Proc Natl Acad Sci U S A, 2015. **112**(38): p. E5281-9.
64. Amadou Amani, S., et al., *Clostridioides difficile Infection Induces an Inferior IgG Response to That Induced by Immunization and Is Associated with a Lack of T Follicular Helper Cell and Memory B Cell Expansion.* Infect Immun, 2020. **88**(3).
65. Holodick, N.E., N. Rodriguez-Zhurbenko, and A.M. Hernandez, *Defining Natural Antibodies.* Front Immunol, 2017. **8**: p. 872.
66. Weller, S., et al., *Human blood IgM "memory" B cells are circulating splenic marginal zone B cells harboring a prediversified immunoglobulin repertoire.* Blood, 2004. **104**(12): p. 3647-54.

67. Keitany, G.J., et al., *Blood Stage Malaria Disrupts Humoral Immunity to the Pre-erythrocytic Stage Circumsporozoite Protein.* Cell Rep, 2016. **17**(12): p. 3193-3205.
68. Chua, C.L., et al., *The neutralizing role of IgM during early Chikungunya virus infection.* PLoS One, 2017. **12**(2): p. e0171989.
69. Devito, C., et al., *Human IgM monoclonal antibodies block HIV-transmission to immune cells in cervico-vaginal tissues and across polarized epithelial cells in vitro.* Sci Rep, 2018. **8**(1): p. 10180.
70. Skountzou, I., et al., *Influenza virus-specific neutralizing IgM antibodies persist for a lifetime.* Clin Vaccine Immunol, 2014. **21**(11): p. 1481-9.
71. Weitkamp, J.H., et al., *Infant and adult human B cell responses to rotavirus share common immunodominant variable gene repertoires.* J Immunol, 2003. **171**(9): p. 4680-8.
72. Foreman, A.L., et al., *B cells in autoimmune diseases: insights from analyses of immunoglobulin variable (Ig V) gene usage.* Autoimmun Rev, 2007. **6**(6): p. 387-401.
73. Jackson, K.J., et al., *The shape of the lymphocyte receptor repertoire: lessons from the B cell receptor.* Front Immunol, 2013. **4**: p. 263.
74. Yamada, M., et al., *Preferential utilization of specific immunoglobulin heavy chain diversity and joining segments in adult human peripheral blood B lymphocytes.* J Exp Med, 1991. **173**(2): p. 395-407.
75. Volpe, J.M. and T.B. Kepler, *Large-scale analysis of human heavy chain V(D)J recombination patterns.* Immunome Res, 2008. **4**: p. 3.
76. Shlomchik, M.J., et al., *The role of clonal selection and somatic mutation in autoimmunity.* Nature, 1987. **328**(6133): p. 805-11.
77. Wu, Y.C., et al., *High-throughput immunoglobulin repertoire analysis distinguishes between human IgM memory and switched memory B-cell populations.* Blood, 2010. **116**(7): p. 1070-8.
78. Lee, Y., et al., *Bezlotoxumab (Zinplava) for Clostridium Difficile Infection: The First Monoclonal Antibody Approved to Prevent the Recurrence of a Bacterial Infection.* P T, 2017. **42**(12): p. 735-738.
79. Chapin, R.W., et al., *Bezlotoxumab: Could This be the Answer for Clostridium difficile Recurrence?* Ann Pharmacother, 2017. **51**(9): p. 804-810.
80. Larabee, J.L., et al., *Exposure of neutralizing epitopes in the carboxyl-terminal domain of TcdB is altered by a proximal hypervariable region.* J Biol Chem, 2015. **290**(11): p. 6975-85.
81. Amanna, I.J., N.E. Carlson, and M.K. Slifka, *Duration of humoral immunity to common viral and vaccine antigens.* N Engl J Med, 2007. **357**(19): p. 1903-15.
82. Sutton, T.C., et al., *In Vitro Neutralization Is Not Predictive of Prophylactic Efficacy of Broadly Neutralizing Monoclonal Antibodies CR6261 and CR9114 against Lethal H2 Influenza Virus Challenge in Mice.* J Virol, 2017. **91**(24).
83. Bootz, A., et al., *Protective capacity of neutralizing and non-neutralizing antibodies against glycoprotein B of cytomegalovirus.* PLoS Pathog, 2017. **13**(8): p. e1006601.
84. Lawrence, S.J., et al., *Clostridium difficile-associated disease treatment response depends on definition of cure.* Clin Infect Dis, 2007. **45**(12): p. 1648; author reply 1649-51.
85. Cohen, N.A., et al., *Clostridium difficile fecal toxin level is associated with disease severity and prognosis.* United European Gastroenterol J, 2018. **6**(5): p. 773-780.
86. Henderson, M., et al., *A Review of the Safety and Efficacy of Vaccines as Prophylaxis for Clostridium difficile Infections.* Vaccines (Basel), 2017. **5**(3).
87. Krivan, H.C. and T.D. Wilkins, *Purification of Clostridium difficile toxin A by affinity chromatography on immobilized thyroglobulin.* Infect Immun, 1987. **55**(8): p. 1873-7.
88. Zheng, G.X., et al., *Massively parallel digital transcriptional profiling of single cells.* Nat Commun, 2017. **8**: p. 14049.

89. Gupta, N.T., et al., *Change-O: a toolkit for analyzing large-scale B cell immunoglobulin repertoire sequencing data.* Bioinformatics, 2015. **31**(20): p. 3356-8.
90. Smith, K., et al., *Rapid generation of fully human monoclonal antibodies specific to a vaccinating antigen.* Nat Protoc, 2009. **4**(3): p. 372-84.
91. Smith, K., et al., *Fully human monoclonal antibodies from antibody secreting cells after vaccination with Pneumovax(R)23 are serotype specific and facilitate opsonophagocytosis.* Immunobiology, 2013. **218**(5): p. 745-54.

834 **FIGURE LEGENDS**

835 **Figure 1. Isolation, sequencing, and repertoire analysis of CTD-specific B_{mem} cells.** (A)
836 Blood samples were obtained from subjects with a history of CDI and used as a source of enriched
837 B cells. (B) Enriched B cells were labeled with a cocktail of fluorochrome-conjugated mAbs and
838 Alexa488-conjugated CTD as described in methods. Pseudocolor plots 1 through 3 depict the
839 gating strategy allowing identification and sorting of $CD19^+$,$CD20^+$,$CD27^+$,$CD38^-$,CTD^+ cells and
840 $CD19^+$,$CD20^+$,$CD27^+$,$CD38^-$,CTD^- cells. Data shown are from subject 1008. (C) Shows frequency
841 of CTD^+ B_{mem} in 3 healthy controls versus 6 previously infected subjects. The subjects included
842 in the single-cell analysis are denoted by red symbols: 1008 (0.34%), 1009 (0.06%) and 1013
843 (0.11%). Black dots denote other subjects recruited: 1012 (0%), 1015 (0.11%) and 1018 (0.19%).
844 The line indicates the mean. A two-tailed unpaired t test with Welch's correction was applied to
845 determine statistical significance in the differences observed (*, $p < 0.05$). (D) Sorted CTD^+ and
846 CTD^- B_{mem} cells were processed as depicted and described in methods, resulting in the
847 generation of individually barcoded and fully sequenced V(D)J regions for each B_{mem} cell. FASTA
848 files were generated using the Cell Ranger 3.0.2 pipeline and the Change-O toolkit was used to
849 analyze the data.

850

851 **Figure 2. Antibody isotype and subclass distribution in B_{mem} cells.** (A) Sequences from
852 CTD^+ B_{mem} cells were analyzed for isotype (top row) and IgG subclass distribution (bottom row).
853 Y axes denote the number of VDJ sequences analyzed, representative of the total CTD^+ B_{mem}
854 cells analyzed. (B) Sequences from CTD^- B_{mem} cells were analyzed as in (A).

855

856 **Figure 3. V gene usage in the Ig heavy chain**. (A) Depicts the V gene usage of CTD^+ (top row)
857 and CTD^- (bottom row) B_{mem} cells from each subject. IgM, IgG, and IgA sequences were included
858 in the analysis. (B) Heat maps depict the heavy chain V-J gene recombination pairs within the
859 VH3 gene family. Sequences from the CTD^+ B_{mem} cells (top panel) and from CTD^- B_{mem} cells

(bottom panel) are shown. Data shown are from subject 1008. The color scale indicates the frequency of occurrence of each VH3-J pair. Pale yellow represents a frequency of zero and blue represents frequencies above zero.

Figure 4. Light chain distribution and their V gene usage in CTD^+ and CTD^- B_{mem} cells. (A) Depicts the number of CTD^+ B_{mem} cells expressing a kappa or a lambda light chain. Numbers above bars denote the kappa / lambda ratio. (B) As in (A) but depicts kappa / lambda ratio for CTD^- B_{mem} cells. (C) The frequency and distribution of V gene usage by the kappa (left) and lambda (right) chains by CTD^+ B_{mem} is shown. (D) Is as in (C), but depicts light chain V gene usage by the CTD^- B_{mem} cells.

Figure 5. Somatic hyper-mutation in CTD^+ and CTD^- B_{mem} cells. (A) Depicts the percent nucleotide mutations as compared to germline. Replacement mutations resulting in an amino acid change and silent mutations resulting in no amino acid change in the heavy chain V regions of IgA, IgG and IgM sequences from CTD^+ B_{mem} cells are presented. (B) Is as in (A) but depicts CTD^- B_{mem} cells. A Kruskal-Wallis test with Dunn's post-test correction was used to determine statistical significance in differences between mutation frequencies observed in each Ab isotype (****, $p < 0.0001$).

Figure 6. Heavy chain V gene usage, somatic hyper-mutation and CDR3 length in $IgG1^+$ B_{mem} cells. (A) Depicts V gene family usage (top), number of replacement mutations (middle) and CDR3 amino acid (AA) length (bottom) for the CTD^+ B_{mem} IgG1 heavy chain sequences. (B) Is as in (A) but depicts IgG1 heavy chain sequences from CTD^- B_{mem} cells.

884 **Figure 7. Clonal expansion in IgM$^+$ Bmem cells.** Graphs depict the clonal expansion in IgM$^+$
885 sequences from (A) CTD$^+$ and (B) CTD$^-$ Bmem cells. The number in the center of each chart
886 denotes the number of sequences analyzed. The numbers in the legends to the right of each
887 chart indicate the size of a given clone. The shaded areas represents the frequency with which
888 clones of each size appeared within the total sample.
889
890 **Figure 8. Bmem-encoded mAbs bind the CTD region of TcdB1 and TcdB2.** Select IgG1
891 heavy and light chain sequences from CTD$^+$ Bmem cells were cloned and transfected into
892 HEK293 cells to generate physiologically paired, full-length human mAbs. (A) TcdB1-CTD-
893 binding by mAbs from subjects 1008 (top), 1009 (middle) and 1013 (bottom) were tested by
894 ELISA. The symbol (#) above a bar indicates the mAbs that were analyzed for CTD-binding
895 affinity. Duplicates from a single experiment are presented and are representative of at least two
896 independent determinations. (B) Is as in (A) except TcdB2-CTD-binding was analyzed. The
897 error bars depict S.E.M.
898
899 **Figure 9. Bmem-encoded mAbs bind CTD with low to moderate affinity.** (A) Select mAbs
900 from 1008 (top) and 1009 (bottom) were subjected to a 16-point dilution curve to calculate their
901 binding constants (*Kd*) to analyze their binding affinity to TcdB1-CTD. The K*d* values are as
902 indicated. (B) Is as in (A) except the binding affinity to TcdB2-CTD for select mAbs from 1009
903 and 1013 was analyzed. Each experiment was performed at least three times with the same
904 results.
905
906 **Figure 10. CTD-specific Bmem encode non-neutralizing antibodies**. (A) Serum from CTD-
907 immunized rabbit diluted to 1:100 and mAbs from subjects 1008, 1009 and 1013 at a final
908 concentration of 10 µg/mL mixed with media containing 0.23 nM TcdB1 were added to CHO
909 cells to assess cell viability. (B) IgG from plasma of subjects 1008, 1009 and 1013 was depleted

and tested *in vitro* for toxin neutralization capacity. The plasma with and without IgG were diluted 1:100 in media with 0.23 nM TcdB1. (C) Is as in A and (D) is as in (B) except samples were mixed with media containing 0.25 nM TcdB2 and added to CHO cells to assess cell viability. Red dotted line represents CHO cell viability in the presence of media containing toxin alone. Duplicates from a single experiment are presented and are representative of at least two independent determinations. The error bars depict S.E.M.

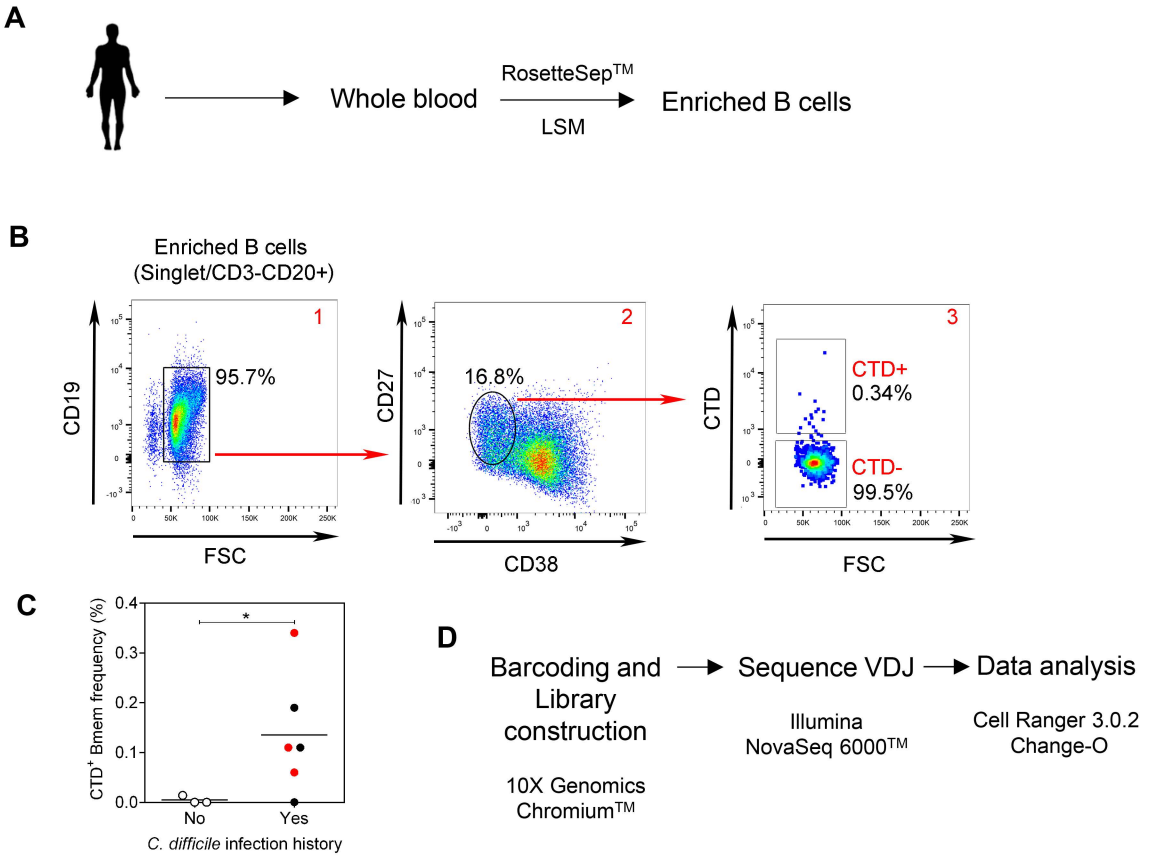

Figure 1. Isolation, sequencing, and repertoire analysis of CTD-specific Bmem cells. (A) Blood samples were obtained from subjects with a history of CDI and used as a source of enriched B cells. (B) Enriched B cells were labeled with a cocktail of fluorochrome-conjugated mAbs and Alexa488-conjugated CTD as described in methods. Pseudocolor plots 1 through 3 depict the gating strategy allowing identification and sorting of $CD19^+$,$CD20^+$,$CD27^+$,$CD38^-$,CTD^+ cells and $CD19^+$,$CD20^+$,$CD27^+$,$CD38^-$,CTD^- cells. Data shown are from subject 1008. (C) Shows frequency of CTD^+ Bmem in 3 healthy controls versus 6 previously infected subjects. The subjects selected for the single-cell analysis are denoted by red symbols: 1008 (0.34%), 1009 (0.06%) and 1013 (0.11%). Black dots denote other subjects recruited: 1012 (0%), 1015 (0.11%) and 1018 (0.19%). The line indicates the mean. A two-tailed unpaired t test with Welch's correction was applied to determine statistical significance in the differences observed (*, $p < 0.05$). (D) Sorted CTD^+ and CTD^- Bmem cells were processed as depicted and described in methods, resulting in the generation of individually barcoded and fully sequenced VDJ regions for each Bmem cell. FASTA files were generated using the Cell Ranger 3.0.2 pipeline and the Change-O toolkit was used to analyze the data.

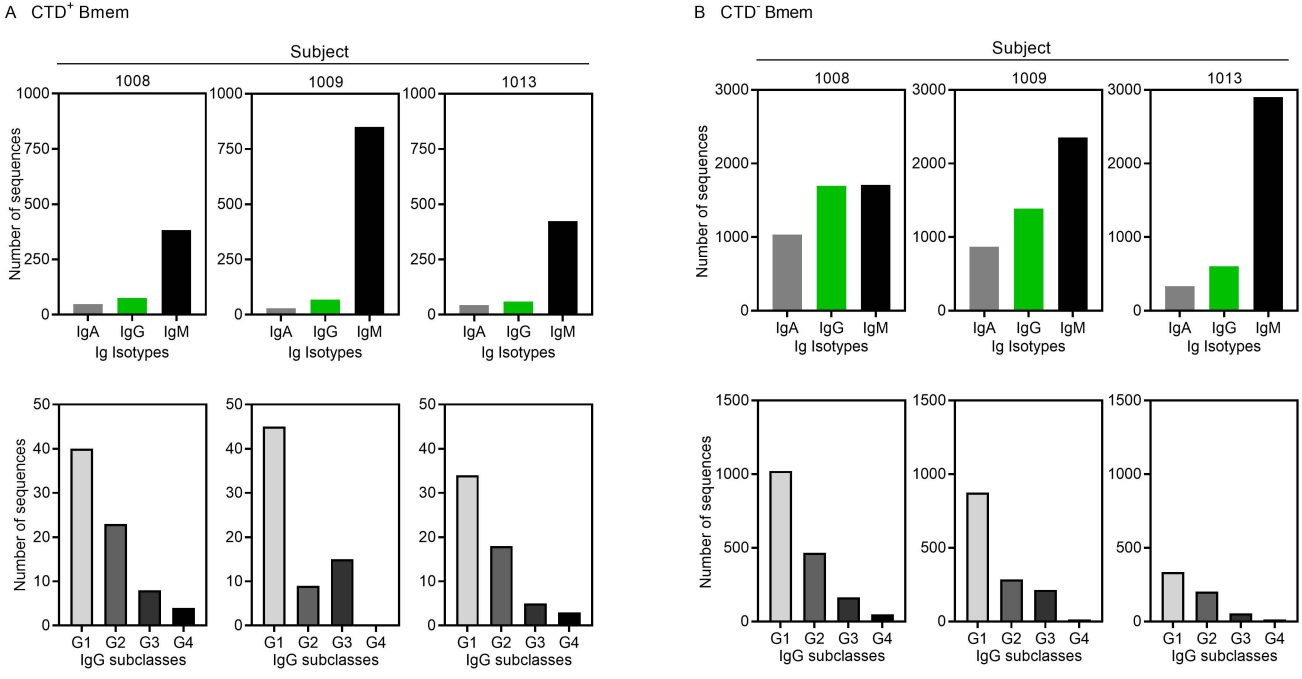

Figure 2. Antibody isotype and subclass distribution in Bmem cells. (A) Sequences from CTD$^+$ Bmem cells were analyzed for isotype (top row) and IgG subclass distribution (bottom row). Y axes denote the number of VDJ sequences analyzed, representative of the total CTD$^+$ Bmem cells analyzed. (B) Sequences from CTD$^-$ Bmem cells were analyzed as in (A).

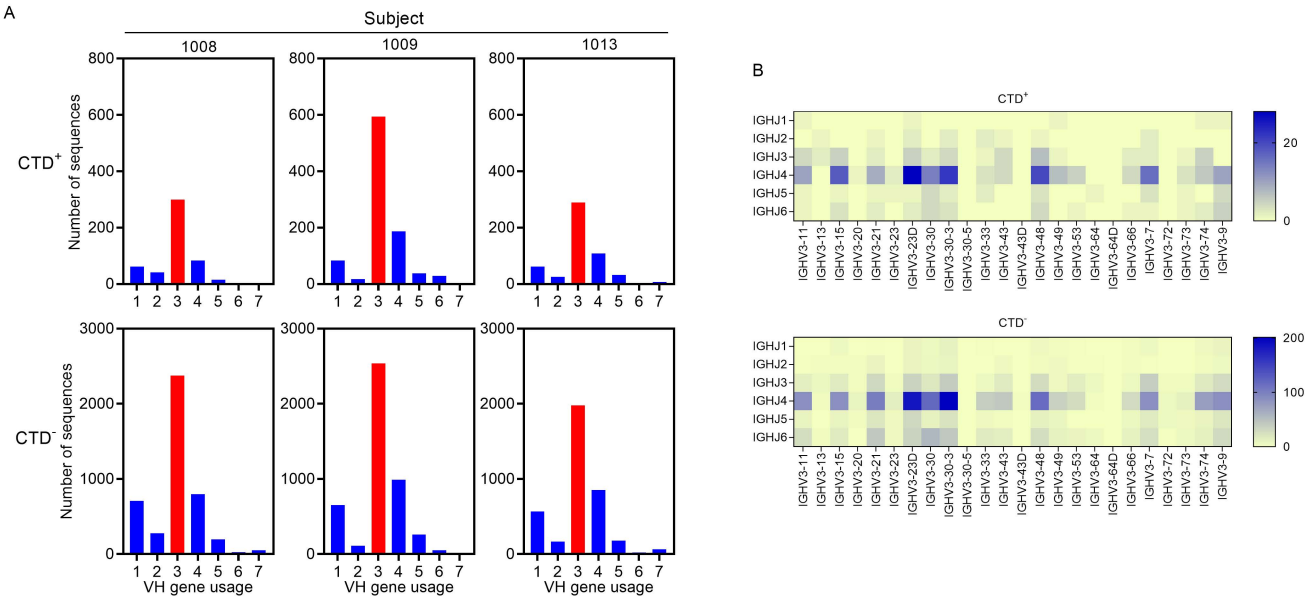

Figure 3. V gene usage in the Ig heavy chain. (A) Depicts the V gene usage of CTD$^+$ (top row) and CTD$^-$ (bottom row) Bmem cells from each subject. IgM, IgG, and IgA sequences were included in the analysis. (B) Heat maps depict the heavy chain V-J gene recombination pairs within the VH3 gene family. Sequences from the CTD$^+$ Bmem cells (top panel) and from CTD$^-$ Bmem cells (bottom panel) are shown. Data shown are from subject 1008. The color scale indicates the frequency of occurrence of each VH3-J pair. Pale yellow represents a frequency of zero and blue represents frequencies above zero.

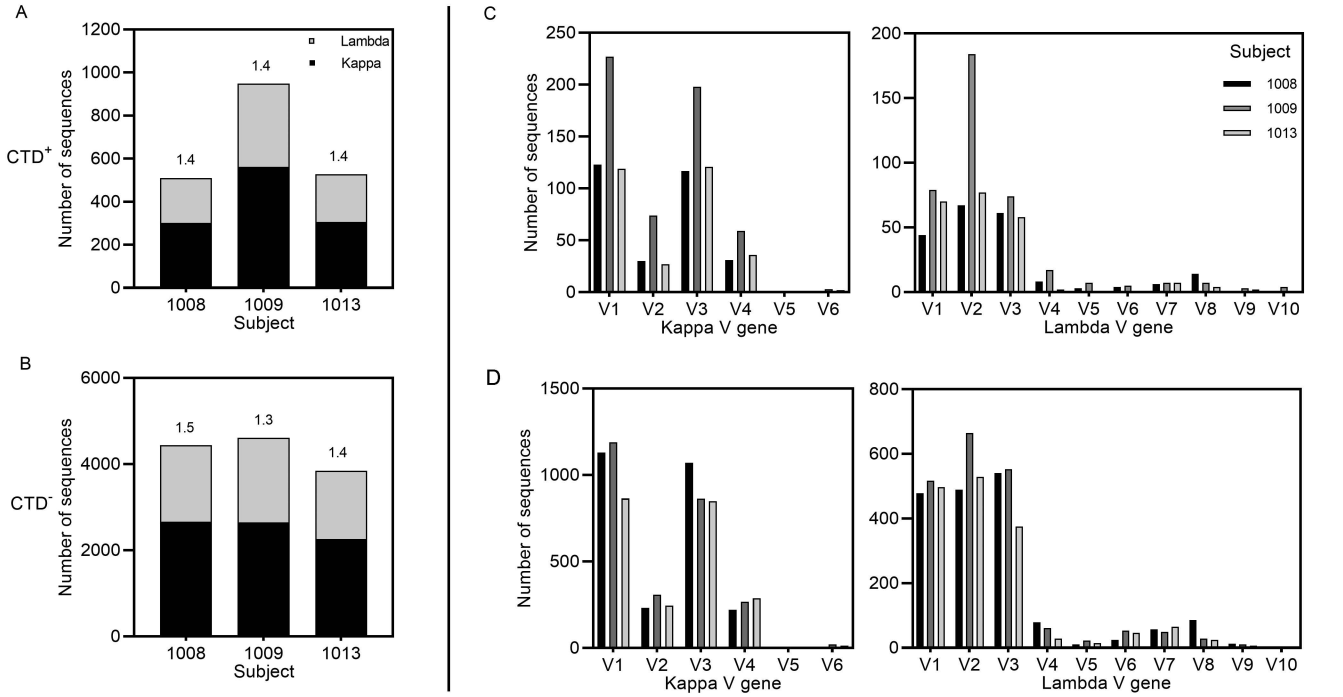

Figure 4. Light chain distribution and their V gene usage in CTD$^+$ and CTD$^-$ Bmem cells. (A) Depicts the number of CTD$^+$ Bmem cells expressing a kappa or lambda light chain. Numbers above bars denote the kappa / lambda ratio. (B) As in (A) but depicts kappa / lambda ratio for CTD$^-$ Bmem cells. (C)The frequency and distribution of V gene usage by the kappa (left) and lambda (right) chains by CTD$^+$ Bmem is shown. (D) Is as in (C), but depicts light chain V gene usage by the CTD$^-$ Bmem cells.

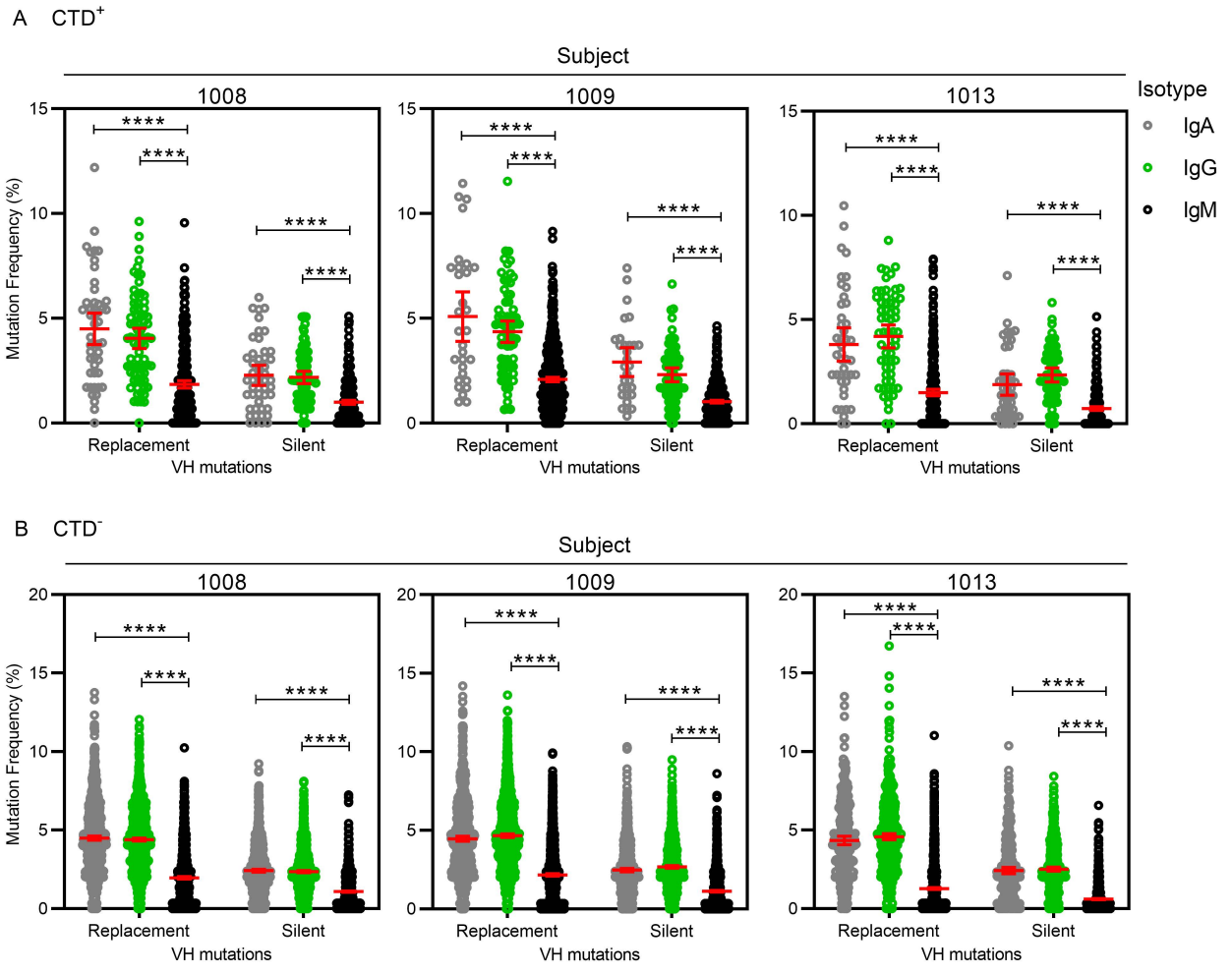

Figure 5. Somatic hyper-mutation in CTD$^+$ and CTD$^-$ B$_{mem}$ cells. (A) Depicts the percent nucleotide mutations as compared to germline. Replacement mutations resulting in an amino acid change and silent mutations resulting in no amino acid change in the heavy chain V regions of IgA, IgG and IgM sequences from CTD$^+$ B$_{mem}$ cells are presented. (B) Is as in (A) but depicts CTD$^-$ B$_{mem}$ cells. A Kruskal-Wallis test with Dunn's post-test correction was used to determine statistical significance in differences between mutation frequencies observed in each Ab isotype (****, p <0.0001).

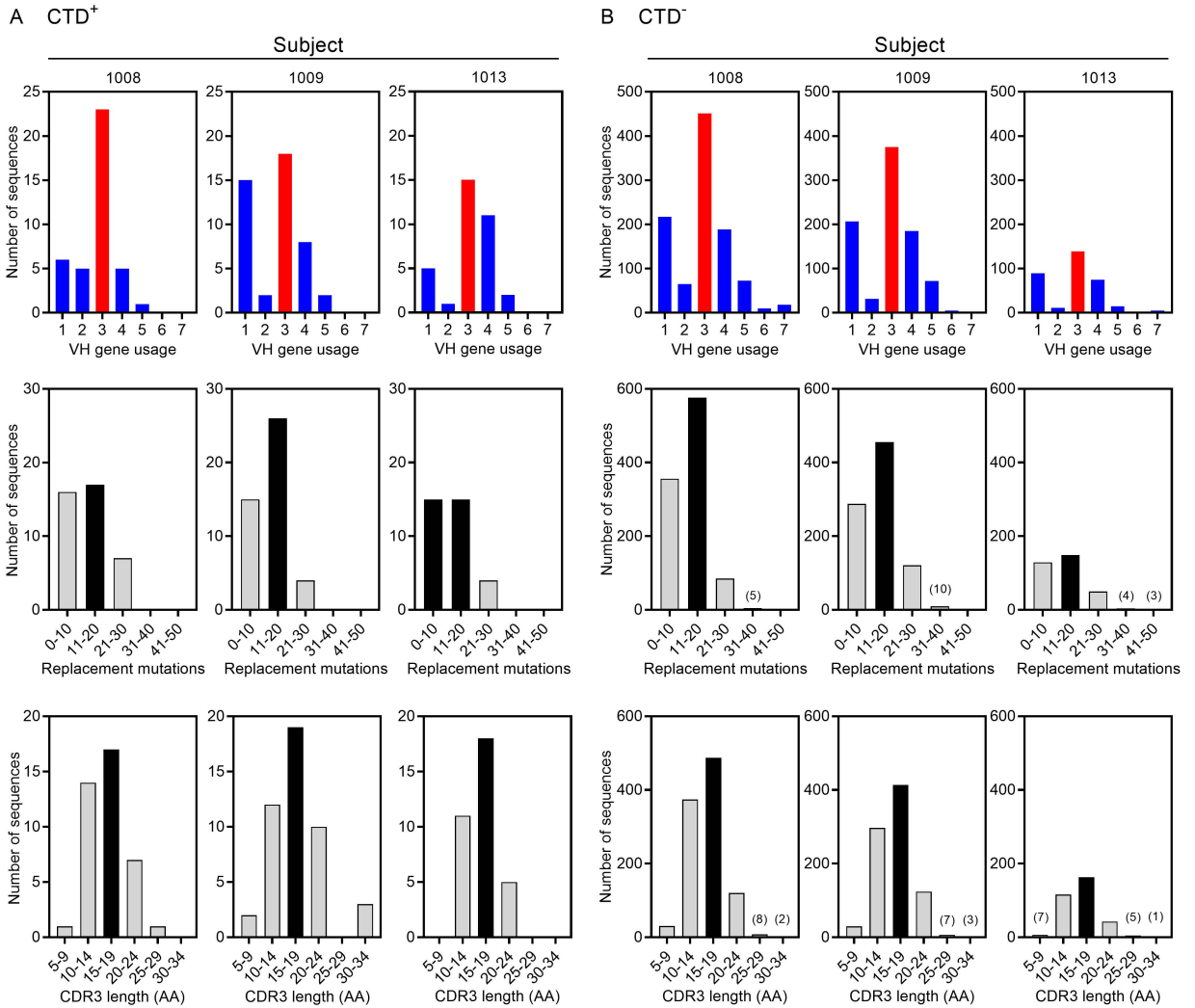

Figure 6. Heavy chain V gene usage, somatic hyper-mutation and CDR3 length in IgG1$^+$ Bmem cells. (A) Depicts V gene family usage (top), number of replacement mutations (middle) and CDR3 amino acid (AA) length (bottom) for the CTD$^+$ Bmem IgG1 heavy chain sequences. (B) Is as in (A) but depicts IgG1 heavy chain sequences from CTD$^-$ Bmem cells.

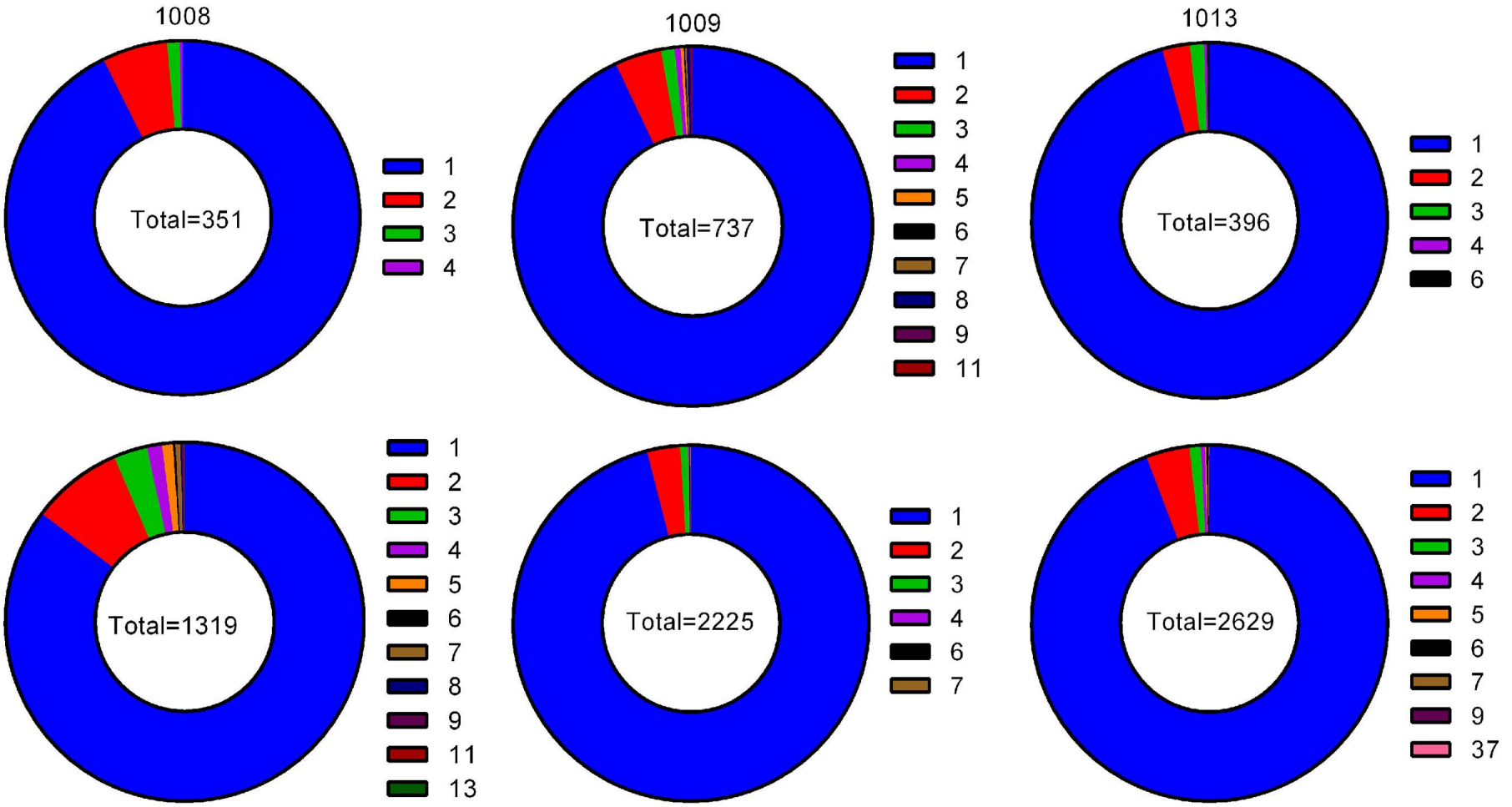

Figure 7. Clonal expansion in IgM$^+$ Bmem cells. Graphs depict the clonal expansion in IgM$^+$ sequences from (A) CTD$^+$ and (B) CTD$^-$ Bmem cells. The number in the center of each chart denotes the number of sequences analyzed. The numbers in the legends to the right of each chart indicate the size of a given clone. The shaded areas represents the frequency with which clones of each size appeared within the total sample.

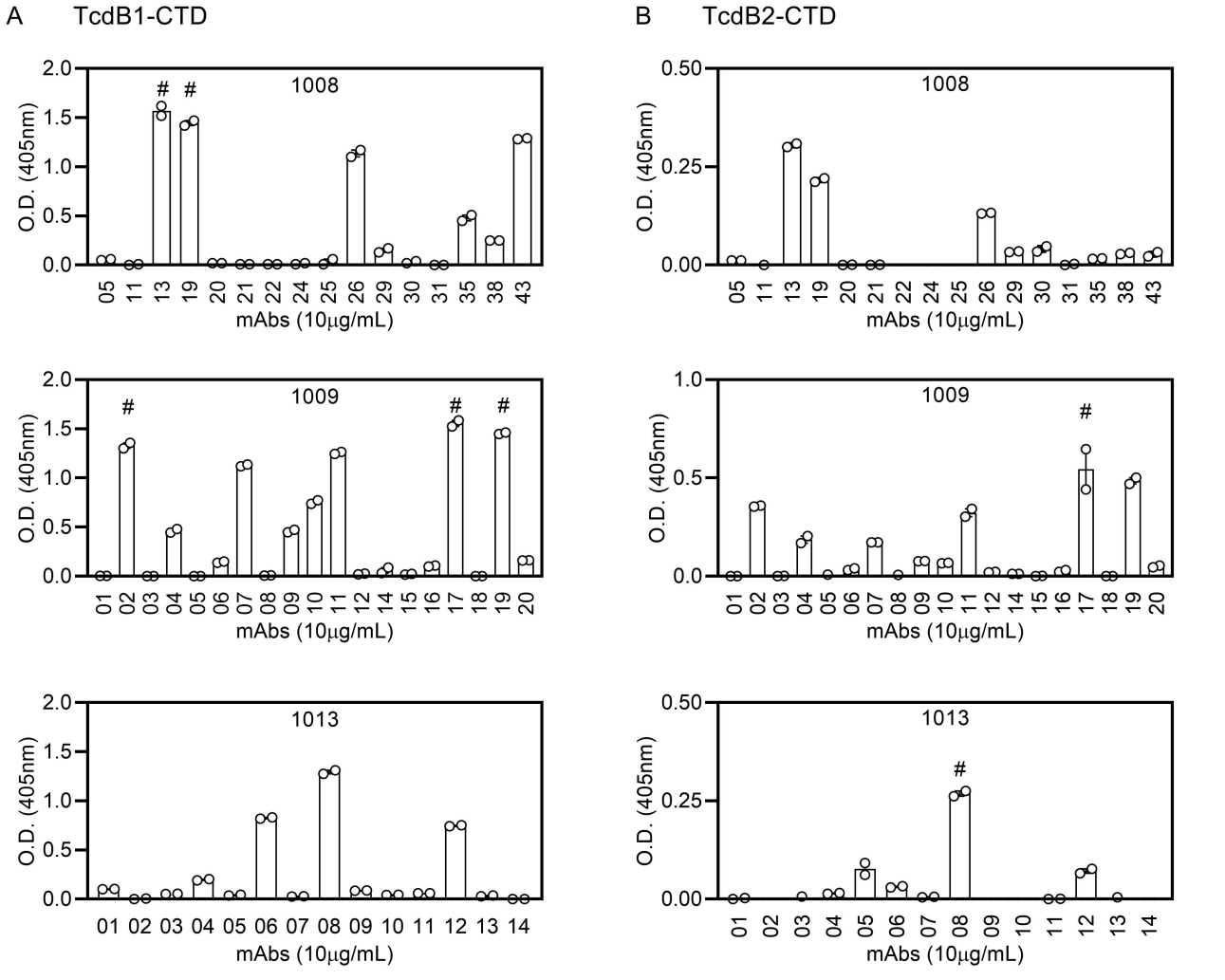

Figure 8. Bmem-encoded mAbs bind the CTD region of TcdB1 and TcdB2. Select IgG1 heavy and light chain sequences from CTD$^+$ Bmem cells were cloned and transfected into HEK293 cells to generate physiologically paired, full-length human mAbs. (A) TcdB1-CTD-binding by mAbs from subjects 1008 (top), 1009 (middle) and 1013 (bottom) were tested by ELISA. The symbol (#) above a bar indicates the mAbs that were analyzed for CTD-binding affinity. Duplicates from a single experiment are presented and are representative of at least two independent determinations. (B) Is as in (A) except TcdB2-CTD-binding was analyzed. The error bars depict S.E.M.

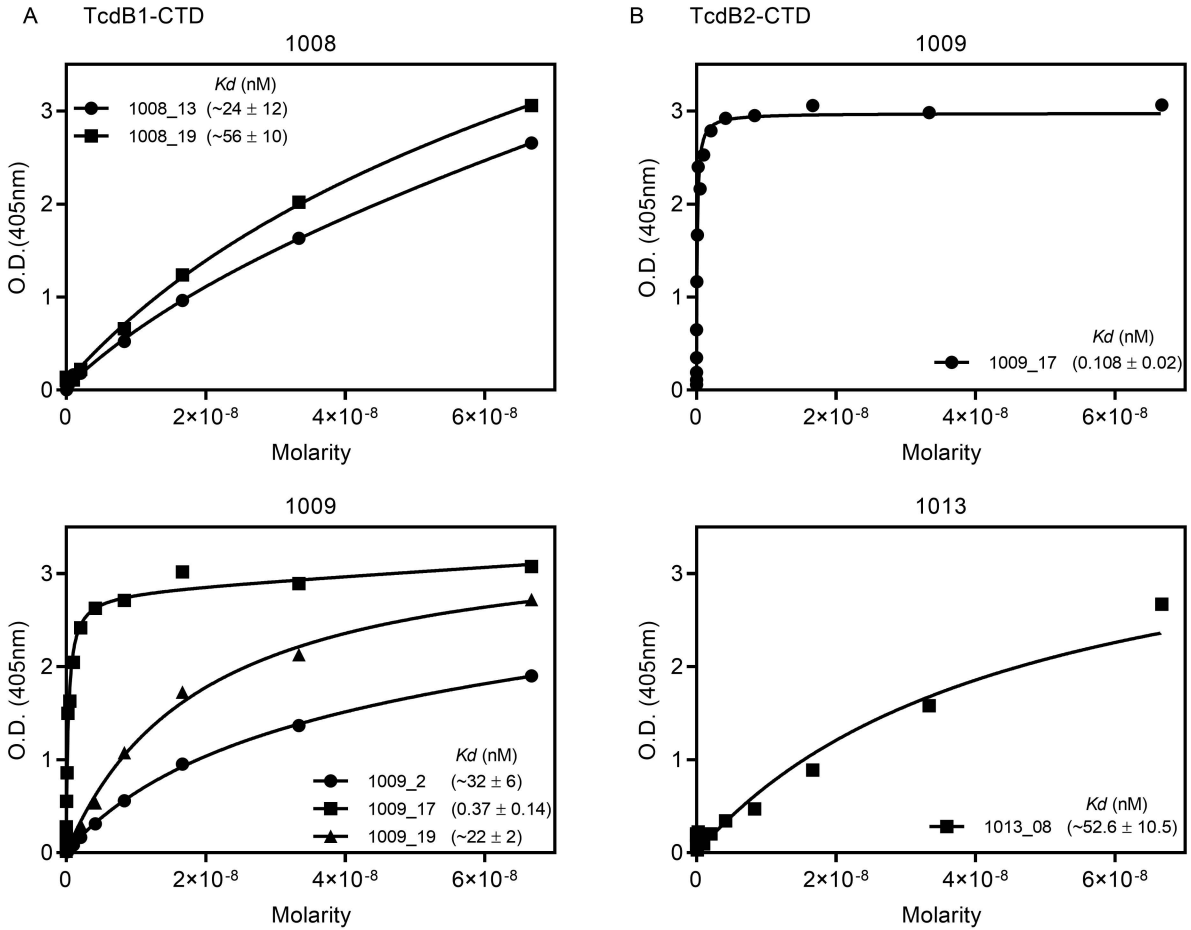

Figure 9. B_{mem}-encoded mAbs bind CTD with low to moderate affinity. (A) Select mAbs from 1008 (top) and 1009 (bottom) were subjected to a 16-point dilution curve to calculate their binding constants (*Kd*) to analyze their binding affinity to TcdB1-CTD. The *Kd* values are as indicated. (B) Is as in (A) except the binding affinity to TcdB2-CTD for select mAbs from 1009 and 1013 was analyzed. Each experiment was performed at least three times with the same results.

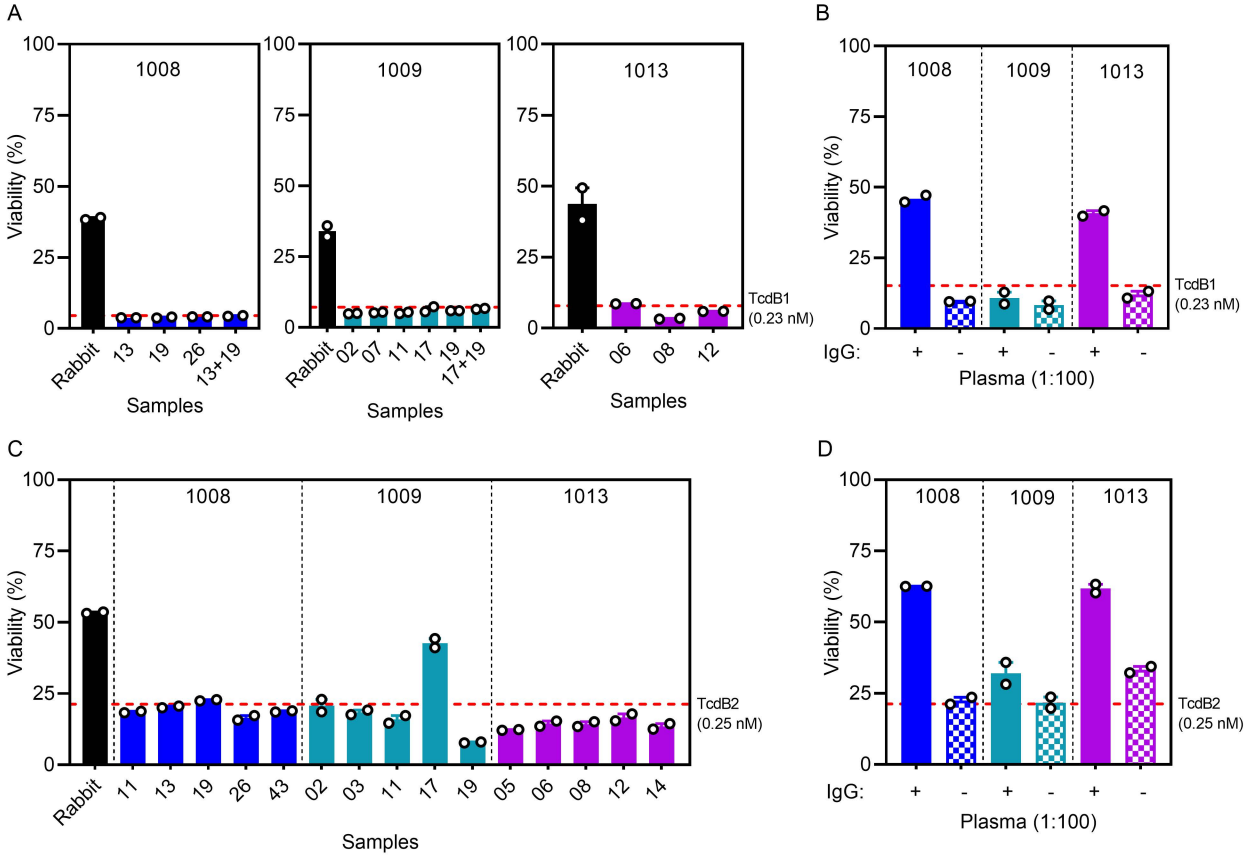

Figure 10. CTD-specific B$_{mem}$ encode non-neutralizing antibodies. (A) Serum from CTD-immunized rabbit diluted to 1:100 and mAbs from subjects 1008, 1009 and 1013 at a final concentration of 10 µg/mL mixed with media containing 0.23 nM TcdB1 were added to CHO cells to assess cell viability. (B) IgG from plasma of subjects 1008, 1009 and 1013 was depleted and tested *in vitro* for toxin neutralization capacity. The plasma with and without IgG were diluted 1:100 in media with 0.23 nM TcdB1. (C) Is as in (A) and (D) is as in (B) except samples were mixed with media containing 0.25 nM TcdB2 and added to CHO cells to assess cell viability. Red dotted line represents CHO cell viability in the presence of media containing toxin alone. Duplicates from a single experiment are presented and are representative of at least two independent determinations. The error bars depict S.E.M.